SINGLE AND BINARY ADSORPTION OF NICKEL AND ZINC IONS FROM AQUEOUS SOLUTIONS USING COIRPITH AS THE ADSORBENT

Eshana Niharika Ranasinghe

(178057H)

Degree of Master of Science

Department of Chemical and Process Engineering

University of Moratuwa

Sri Lanka

December 2020

SINGLE AND BINARY ADSORPTION OF NICKEL AND ZINC IONS FROM AQUEOUS SOLUTIONS USING COIRPITH AS THE ADSORBENT

Eshana Niharika Ranasinghe

178057H

Thesis submitted in partial fulfillment of the requirements for the Degree of Master of Science - Major component by Research

Supervisor: Prof. (Mrs.) B.M.W.P.K. Amarasinghe

Department of Chemical and Process Engineering
University of Moratuwa
Sri Lanka

December 2020

DECLARATION OF THE CANDIDATE & SUPERVISOR

I declare that this is my own work and this thesis does not incorporate without acknowledgement any material previously submitted for a Degree or Diploma in any University or other institute of higher learning and to the best of my knowledge and belief it does not contain any material previously published or written by another person except where the acknowledgement is made in the text.

Signature:…….. Date:……

E.N. Ranasinghe

I hereby grant the University of Moratuwa the right to archive and to make available my thesis in whole or part in the University Libraries in all forms of media subject to the provisions of the current Copyright Act of Sri Lanka. I retain all proprietary rights, such as patent rights. I also retain the right to use in future works (such as articles or books) all or part of this thesis.

Signature:…….. Date:……

E.N. Ranasinghe

I have supervised and accepted this thesis for the award of the degree.

Signature of the Supervisor:…… Date:……

Prof. (Mrs.) B.M.W.P.K. Amarasinghe

Abstract

This study analysed the competitive adsorption of multicomponent systems onto coir pith, readily available and environmentally friendly adsorbent chosen for the study. The efficacy of unmodified coir pith as an adsorbent as well as its physical and chemical characteristics were studied to analyse single and binary systems of nickel and zinc adsorption onto coir pith as well as the effects of temperature, concentration, adsorbent dose and pH to determine the optimal conditions for adsorption.

The equilibrium data for the single system adsorption of nickel and the single system adsorption of zinc at 30 °C was analysed using the Langmuir and Freundlich isotherm models while the multicomponent adsorption was analysed using the Langmuir, the Freundlich, the competitive Langmuir, the non-competitive Langmuir, the modified competitive Langmuir and the Langmuir Freundlich isotherm models. The single system adsorption data for both nickel and zinc fit the Freundlich model which showed the adsorption surface was heterogeneous. The multicomponent adsorption system data fit the Langmuir isotherm model the best which showed the adsorption surface formed a monolayer.

Most adsorption occurs at a higher pH value. To decrease costs and possibility of metal hydroxide precipitation the adsorption should be carried out at a neutral pH.

The kinetics of single system and binary system adsorption of nickel and zinc was studied using Lagergren pseudo first order model, pseudo second order model and the intraparticle diffusion model. The experimental data showed all of the systems could be described using pseudo second order model which shows adsorption occurs primarily through chemisorptions. In the single system the coir pith had a higher capacity for zinc than nickel. In the single system adsorption of nickel the adsorption increases with temperature which shows the adsorption of nickel is an endothermic process. In the zinc single systems the adsorption decreased when temperature increased which shows zinc adsorption is an exothermic process. In the adsorption capacity in the binary system is less than either of the single systems which prove in the presence of competitive species metal ion adsorption is hindered.

The data was analysed using the Intraparticle diffusion model which showed intraparticle diffusion in the nickel single system and in the zinc single system at 30 °C but little to no intraparticle diffusion at higher temperatures or in the multicomponent system

The FTIR analysis of the surface of coir pith before and after adsorption shows that adsorption decreases the presence of hydroxyl (-OH) bonds. This confirms the results of the kinetic analysis that the adsorption is a chemical process which breaks and forms bonds with the functional groups on the coir pith surface. The metal ion forms a complex with the polar surface functional groups during adsorption and the metal ion remains bonded to the surface even when the adsorbent is removed from the water and dried.

This confirms coir pith is an effective adsorbent for the removal of heavy metals from aqueous solution. To optimise multicomponent adsorption of nickel and zinc it should be carried out close to 30 °C in a solution of neutral pH and allowed to reach equilibrium.

TABLE OF CONTENTS

LIST OF FIGURES

LIST OF TABLES

LIST OF ABBREVIATIONS

q_e	equilibrium adsorption capacity(mg g^{-1})
q_{max}	maximum adsorption capacity corresponding to complete coverage of available sites (mg g^{-1})
C_e	equilibrium concentration of metal ions in solution (mg L^{-1})
k_L	Langmuir isotherm constant (L/mg).
k_F	Freundlich constant which is the relative adsorption capacity of the adsorbent
n	Freundlich constant which indicates adsorption intensity
k_1	Lagergren pseudo first order adsorption rate constant
q_t	amount of solute adsorbed on the surface at time t (mg g^{-1})
k_2	Lagergren pseudo second order rate constant of adsorption (g mg^{-1} min^{-1})
h	Initial rate constant (mg g^{-1} min^{-1})
k_{id}	rate constant of the Intraparticle diffusion model
c	constant which is proportional to the boundary layer thickness
k_d	equilibrium dissociation constant
ΔG^o	change in free energy(J mol^{-1})
ΔH^o	standard enthalpy
ΔS^o	standard entropy
T	temperature (K)
R	gas constant (8.314 J mol^{-1} K^{-1})
IUPAC	International Union of Pure and Applied Chemistry
FTIR	Fourier transform infrared spectrometer
SEM	scanning electron microscopy
ICP-MS	inductively coupled plasma mass spectrometry

Acknowledgements

I take this opportunity to express my sincere gratitude to everyone who helped me in numerous ways to complete my research project.

First of all I must thank my supervisor, Prof (Mrs.) B.M.W.P.K. Amarasinghe for supervising my research project. I would not have been able to complete my thesis without her kind guidance, advice, and assistance throughout my research project. I will always be grateful for your kindness and support.

I would like to thankfully acknowledge all the members of the academic staff and technical staff of the Department of Chemical and Process Engineering. In particular, Dr. (Mrs.) S.H.P. Gunawardena, and Prof. S Walpolage, Heads of the Department during my research, and Prof. P.G. Ratnasiri and Dr. (Ms.) M.Y. Gunasekara for their valuable comments and guidance during my progress reviews.

I gratefully acknowledge the technical support staff of the Environmental Laboratory in particular, Ms. P.D.M. Rodrigo, Technical Officer in Charge of the Laboratory. Your support and assistance made this research a reality.

I would like to thank the Materials Engineering Deptartment for helping me by carrying out SEM and FTIR analysis for me which was integral to my research. I would also like to thank the University SRC grant for funding my research.

Last but not least, I am grateful to my parents for their patience and loving support when I was busy with my research project.

CHAPTER 1: INTRODUCTION

1.1 Background

In recent years there has been an increase in research on adsorption to remove heavy metals, many of which focus on very toxic heavy metals such as arsenic, cadmium and lead. While these metals are important it is also important to study less toxic but still very dangerous metals such as manganese, zinc, and nickel. Nickel and zinc are trace metals in fertilizers and pesticides which build up in soil and water ways over time. Nickel and zinc are also widely used in electroplating, the waste water of which is often introduced directly into rivers. Most of the research also focuses primarily on single system adsorption and batch experiments. While this research is useful it does not accurately replicate waste water which contains a mixture of different compounds where there will be competitive adsorption.

1.2 Research Problem

It is important to develop a system to remove dangerous pollutants from water especially in developing countries which is efficient and simple to carry out and affordable at both large and small scales. Adsorption is seen as a viable method due to its ease of application. The main cost in this process is the adsorbent. Hence, the chosen adsorbent to be used in developing countries should ideally be affordable, readily available and environmentally friendly.

1.3 Research Objectives

The main aim of this research is to study the competitive adsorption of multicomponent systems onto areadily available and environmentally friendly adsorbent. Coir pith was the chosen adsorbent.

The objectives of the research are to;

1. Understand the adsorption process.

2. Study the efficacy of unmodified coir pith as an adsorbent as well as its physical and chemical characteristics.

3. Analysesingle and binary systems of nickel and zinc adsorption onto coir pith as well as the effects of temperature, concentration, adsorbent dose and pH.

4. Determine the optimal conditions for adsorption.

1.4 Structure of the Report

The next chapter describes the literature review done on adsorption, adsorbent and nature of the metal ions. The third chapter describes the research methodology adopted for this study. The fourth chapter discusses the data collections, results and the analysis for the research study. The final chapter contains the conclusions.

CHAPTER 2: LITERATURE REVIEW

2.1 Overview

Increased industrial activity and poor adherence to proper precautions have lead to increased industrial pollution which introduces toxic chemicals and heavy metals into rivers and soil. Pollution of fresh water systems can affect plants, aquatic life as well as the people whose main sources of water are being polluted. Heavy metal ions dissolved in water can be dangerous if present in high enough concentrations. Therefore it is important to develop a system to remove these dangerous pollutants from water which is both efficient, simple to carry out and affordable at both large and small scales.

This chapter reviews the literature under following sections Heavy Metals, Removal of Heavy Metals, Isotherm models, Kinetic models and thermodynamic analysis. The summary section identifies the gap that requires this study.

2.2 Heavy Metals

Heavy metals refer to metals with a relatively high density of greater than 5 g cm^{-3}. This includes most metals and all transition metals. Heavy metals are found abundantly in natural sources such as in water, soil or organisms. Most often they exist as sediment or suspended in the water. While in their natural state, most metals are not dangerous.

Transition metals are defined by IUPAC (Gold Book, 1997) as elements whose atoms have partially filled d-sub-shell, or which can give rise to cations with an incomplete d-sub-shell. These metals show variable valency, have the ability to form complexes which are often coloured. Transition metals in the same period have similar sized ions and sometimes have similar chemical behaviour. Transition metals are used in every part of industry, from construction to manufacturing to agriculture and technology. They are also essential for human life, small amounts of various transition metals are utilised in biological processes. However when the concentration of these metals are too high in the body it can become toxic.

Heavy metals can be introduced into the environment by a variety of ways, such as through industrial waste being introduced directly into rivers, agricultural runoff, domestic waste etc. Industries such as electroplating, electronics and mining can pollute rivers with their untreated waste water. Fertilizers and pesticides often contain heavy metals as well as electronics which have not been correctly disposed of can contribute to pollution.

Heavy metal pollution of zinc can be from galvanised material from roofing, pipes and buckets. The Handbook of the toxicology of metals by Frieberg et al. (1986) details how cadmium which normally exists as bottom sediment and sediment particles, change in the acidity of the water which can cause more cadmium to dissolve in the water. Water which is softer (more acidic) can have higher concentration of cadmium in wells, and acidic water can corrode galvanised pipes which leach heavy metals such as zinc and cadmium into the water.

Elements such as copper and zinc are essential for the physiological processes in all living organisms including micro-organisms and plants. Heavily cultivated soils can suffer from a lack of zinc and copper which requires the use of fertilizers enriched with these elements. Run off from these agricultural sites can lead to its spreading to the environment. Studies by Wyszkowska et al. (2012) have shown that excessive amounts of these elements can result in the disruption of biological processes in plants and microorganisms especially when zinc accumulates in excessive amounts in plants and animals it can hinder copper being absorbs resulting in copper deficiencies.

Nickel is used for metal alloys, manufacture of magnetic material, and manufacture of batteries. It is released into the environment as a result of mining and during burning of fossil fuels for energy generation. In recent years there has been an increased interest in the manufacture of electric cars of which one of the major components is nickel. As this trend increases as will the pollution from nickel mining as well as leaching of nickel from the battery waste.

Nickel can be absorbed into the human body by skin contact through touching material containing nickel such as galvanised material and jewellery as well as by

consuming contaminated food and water. The nickel absorbed is likely not in high enough concentration to cause any harm other than mild skin irritation (Agency of Toxic substances and Disease registry, 2005). The toxicity will depend more on the nickel complex rather than the concentration of the metal itself. Nickel is a mild carcinogen and there have been cases where nickel inhalation has lead to lung cancer, but these have only been due to occupational exposure in factories.

Research by Saleem et al. (1998) has showed the main sources of heavy metal pollution in coastal areas of Karachi are sewage and industrial waste.

According to the National Environmental (Protection and Quality) Regulations (2008) the tolerance limit for nickel and zinc concentrations in industrial and domestic discharge are shown in table 1.

Table 1 Tolerance limits for the discharge of industrial/ domestic waste in Sri Lanka

Maximum Tolerance Limits/ mg L^{-1}	**Nickel**	**Zinc**
Industrial and Domestic waste discharge to inland surface	3.0	2.0
Industrial and Domestic waste discharge to marine coastal	5.0	5.0
Waste water from textile industry being discharged into inland	-	5.0
Effluents into public sewers with central treatment plants	3.0	5.0

Source: National Environmental (protection and quality) regulations (2008) of Sri Lanka

In a study by Wijeyaratne (2016) it was found that the shallow sediments of the Bolgodalake had heavy pollution of nickel, chromium, copper according to numerical sediment quality guidelines of USEPA.

2.3 Removal of Heavy Metals

It is very important to prevent pollution of rivers and soil by waste water from industry and domestic waste. Ideally the dangerous heavy metals and chemicals should be removed from waste water before it is introduced into the environment. There are several methods that can be utilised to remove heavy metals, and the method applied should depend on the conditions of the water, degree of pollution and other financial and material limitations.

An effective method of removing impurities from water is by using reverse osmosis where high pressure is used to force polluted water through a semi-permeable membrane. This keeps impurities on one side of the membrane and allows pure water to pass to the other side. In a study by Bakalár et al. (2009) this method was shown to be best when the solution has a low concentration of impurities as at higher concentrations higher pressure is necessary. However this method can be expensive as it requires expensive equipment and specialised training to carry out. It is difficult to economically purify large amounts of water with this method.

Precipitation is a viable method to remove heavy metals. In a study by El Samrani et al. (2008) heavy metals such as copper, zinc and lead were removed from combined sewer overflow using coagulants such as iron (III) chloride or polyaluminium chloride. Lime solution was shown to be an effective for chemically coagulating and precipitating zinc, cadmium and manganese by increasing the pH of the solution to above pH 9 in a study by L. Charerntanyarak (1999). Recently there have been studies about precipitation using photocatalysis e.g. E. T. Wahyuni et al. (2015) which uses titanium dioxide. Titanium dioxide is a photosensitizer and a semi-conductor which reduces the metal ions and precipitated the metal out of solution. The main drawback is the cost of the coagulants.

Ion exchange is a reversible process where ions between the solution and the surface of the solid substrate. Often a resin with cross-linked structure and multiple functional groups are used in column through which the solution is passed through. (Dąbrowski et al. 2004) The metal ion would ideally exchange with a proton (H^+ ion) on the surface functional group. Ideally the substrate should be re-usable after being treated or washed with an acid solution which should remove the metal ions from its surface.

Electrodialysis uses membranes which are only permeable to either cations or anions. A direct potential is used to separate the cations and anions from each other as well as from the non-charged species in the solution. (Abo-Ghander et al. 2008)

One method of removing these heavy metals which is appealing due to its ease of application is adsorption, where the pollutant is adsorbed onto the adsorbent and then

filtered out with the solid adsorbent. The efficacy of the adsorbent depends on the surface chemistry and structure of the adsorbent. Ideally the adsorbent should be both cheap and readily available.

Adsorption is where a substance, a gas, liquid or dissolved material adheres onto the surface of a solid. Physisorption is a physical adhesion onto a surface driven by attractive intermolecular forces where there is no change in the chemical bonding. Chemisorption is an adhesion where a chemical reaction takes place after a physical adhesion where a chemical bond, either covalent or ionic, is formed between the substance and the surface. Both physisiorption and chemisorptions are reversible but physisoprtion is generally weaker than chemisorptions Oura et. al. (2003).

Graphene is a carbon based nanomaterial with large specific surface area and high chemical stability, (Gopalakrishnan et al. 2015). It has high surface area and can be altered by oxidation to add more hydrophilic functional groups, which makes it a very efficient for the adsorption of heavy metals. (Thangavel et al. 2014)

Activated carbon is porous with a high surface area. It can be made from any high carbon content material. Activated carbon made from coal is expensive but it can be made more cost effective if it is made from agricultural biowaste such as saw dust, coconut shells or wood (Karthikeyan et al. 2005, Babel et al. 2004). Activated carbon is not a selective adsorbent and can adsorb most pollutants irrespective of charge or chemical composition.

Carbon nanotubes are chemically similar to graphene but in a tubular shape rather than a sheet. It can be a single layer or several layers (Hongjie Dai. 2002). Carbon nanotubes have a large surface area, good stability, mesoporous and favourable electrical properties. Adsorption can occur inside pore, on the external surface of the nanotube or between tubes when they are in clusters (Agnihotri et al. 2006). They can be made by arc discharge, laser ablation and flame synthesis. It is very expensive as it requires expensive material or high temperatures and it is difficult to get pure carbon nanotubes as allotropes such as fullerene or grapheme sheets are also produced as by-products.

Clay has a high surface area, good physical properties such as plasticity and good bond strength as well as favourable chemical properties such as a large zeta potential, cation exchange capabilities. It also has good load bearing strength and is resistance to both physical and chemical wear (Singh et al. 2001, Krikorian& Martin, 2008). Bentonite clay is low cost with good ion exchange capacity and regeneratablity. When the clay was heat treated at 400-500 ^{o}C under limited supply of air the structure and water absorption was altered without changing its composition or morphology allowing it to be used in fixed bed columns without expansion. After being used to remove heavy metals the clay can be regenerated using a NaCl/HCl solution at a low pH which removed the adsorbed metal ions via ion exchange.

Zeolites are microporous hydrated aluminosilicate minerals where some of the silica atoms have been replaced with aluminium molecules in the silica lattice. This gives the material an overall negative charge which is balanced out by exchangeable cations (Wingenfelder et al. 2005). This makes it ideal for the adsorption of heavy metal ions. It has a high surface area, good ion exchange properties, very hydrophilic, and has good chemical stability at low pH.

Mesoporous silica has a uniform hexagonal array of channels, with pore size diameter between 2-10 nm which provides a large surface area for adsorption to take place. (Bhattacharyya et al. 2006) It has several polar groups (Si-OH) onto which the metal ions can undergo chemisorption. Its capacity can be improved by chemically adding carboxylic and sulfonic acid groups. The size of the pores can be tailored to the metal ion improving selectivity. However the production of mesoporous silica is laborious and requires specialised chemicals which would make producing large amounts of this for adsorption very expensive.

A cheap alternative is to use agricultural biowaste such as rice husks, vegetable peel, straw, or coir pith as bioadsorbents. In a study by Amarasinghe (2007, 2011) coir pith and tea waste was shown to have a higher capacity for metals such as lead compared to activated carbon.

In a review by Nassrulla et al. (2016) it was shown that lignin can be a good nonspecific adsorbent to remove heavy metal pollutants from waste water. Ho et al. (1999) showed peat was an effective adsorbent in the removal of nickel and copper ions from aqueous solutions. A study by Amarasinghe (2011) showed that coir pith can be used to remove heavy metals lead and cadmium from waste water. Coir pith is shown to be a good non-specific adsorbent in literature as shown in table 2. It can adsorb a variety of metal ions and can either be chemically modified or made into activated carbon to improve its absorption capabilities.

Table 2 Adsorption capacities of various metal ions onto coir pith from literature

Metal ion	**q_{max} (mg g^{-1})**	**References**
Chromium ion/ Cr(VI)	42.71 (57%)	P. Suksabye et al. (2009)
Nickel ion/ Ni(II)	24.39 (80%)	Ratan et al.(2016)
Nickel ion/ Ni(II)	9.5 (41.5%)	A. Ewecharoen et al. (2008)
Cadmium/ Cd(II)	93.4	Kadirvelu, et al. 2003
Cobalt/ Co(II)	12.82	Suksabye P, et al. (2007)
Chromium/ Cr(III)	11.56	
Nickel/ Ni(II)	15.95	
Zinc/ Zn(II)	8.6	Conrad, et al. (2007)
Lead/ Pb(II)	18.9	
Chromium/ Cr(IV)	6.3-26.8	Gonzalez et al. (2008)
Lead ion/ Pb(II)	19.9 (99.8%)	Amarasinghe et al. (2007)

Coir pith has also been shown to be a good adsorbent of nickel and zinc ions compared to other adsorbents in literature having a good q_{max} value and high removal percentage as shown in table 3 and table 4.

Table 3 Adsorption capacities of nickel ions onto coir pith and other adsorbents from literature.

Adsorbent	**Nickle (II)**	
	q_{max} (mg g^{-1})	**References**
Sugar beet pulp	17.5	Reddad, et al.(2002)
Anearobic biomass	25	Hawari, et al.(2006)
Grape stalks	30	Villaescusa, et al. (2004)
Coir pith	9.5 (41.2%)	Ewecharoen et al. (2008)
Modified coir pith	38.9 (94.5%)	Ratan et al.(2016)
Coir pith	24.39	Ajmal et al. (2006)
Testa of groundnut shell	18.79	
Bagasse fly ash	12.82	Taha et al. (2006)

Banana peel	6.88	Annadurai , et al.(2002)
Orange peel	6.01	Malkoc, et al.(2005)
Tea factory waste	15.26	Gosset et al.(1986)
Eutrophic peat	11.15	

Table 4 Adsorption capacities of zinc ions onto coir pith and other adsorbents from literature.

Adsorbent	**Zinc (II)**	
	q_{max} (mg g^{-1})	**References**
Pseudomonas	8.13	Hidayati, et al. (2014)
Zeolite	4.11	Zendelska et al. (2014)
Coir	8.6	Conrad et al. (2007)
Sugar beet pulp	18	Reddad et al. (2002)
Papaya wood	14	Saeed, et al. (2005)
Teakwood sawdust	11	Shukla, et al. (2005)
Groundnut shells	7.6	
Waste Olive cake (untreated)	22	Fernando et al. 2009
Waste Olive cake (treated)	27	
Bentonite (bacteria enriched)	198.76	Jablonovská et al. 2006
Zeolite (bacteria enriched)	88.26	
Quartz sand (bacteria enriched)	92.83	

Multicomponent adsorption is when absorption occurs in a solution where more than one compound can get absorbed onto the adsorbent. Competitive adsorption is when the compounds compete over the same adsorption sites and non-competitive adsorption is when the compounds adsorb onto different sites on the adsorbent. The presence of other compounds in the solution can lead to suppression or promotion of adsorption or the compounds may not affect the adsorption of the others.

In a study by S. N. D. C. Ramos et al. (2015) about the mutlicomponent adsorption of cobalt (II), copper (II) and nickel (II) onto modified sugarcane bagasse, the adsorption of cobalt (II) and nickel (II) was suppressed by the presence of copper (II) while the adsorption of nickel (II) was suppressed by the adsorption of cobalt (II).

2.4 Isotherm models

An adsorption isotherm is a plot of equilibrium adsorption capacity, q_e (mg g^{-1}) against equilibrium concentration, C_e (mg L^{-1}) at a constant temperature. Depending on the adsorbent, substance and other conditions such as pH, the isotherm can have

different shapes. Type I isotherm is when there is a monolayer formation, where the surface adsorption sites are completely covered with a single layer of the adsorbing substance. When the line plateaus the adsorbent has been completely saturated. This is characteristic of microporous solids. Type II isotherm is when following monolayer formation there is a multilayer build up. This is common for non-porous or macroporous adsorbents. Type III isotherm is when there is unrestricted multilayer formation where complete coverage/monolayer does not necessarily occur before multilayers occurring. This occurs when the attraction between the adsorbed ions / molecules are greater than or equal to the attraction between the surface and the ion / molecules. Type IV and type V is when the adsorption occurs on mesoporous solids by multilayer adsorption followed by capillary condensation. Capillary condensation is when vapour adsorbs onto a porous solid where the pore is filled with condensed liquid. Type IV has multilayer formation following monolayer formation while type V has unrestricted multilayer formation. Figure 1 shows type I-type V isotherms.

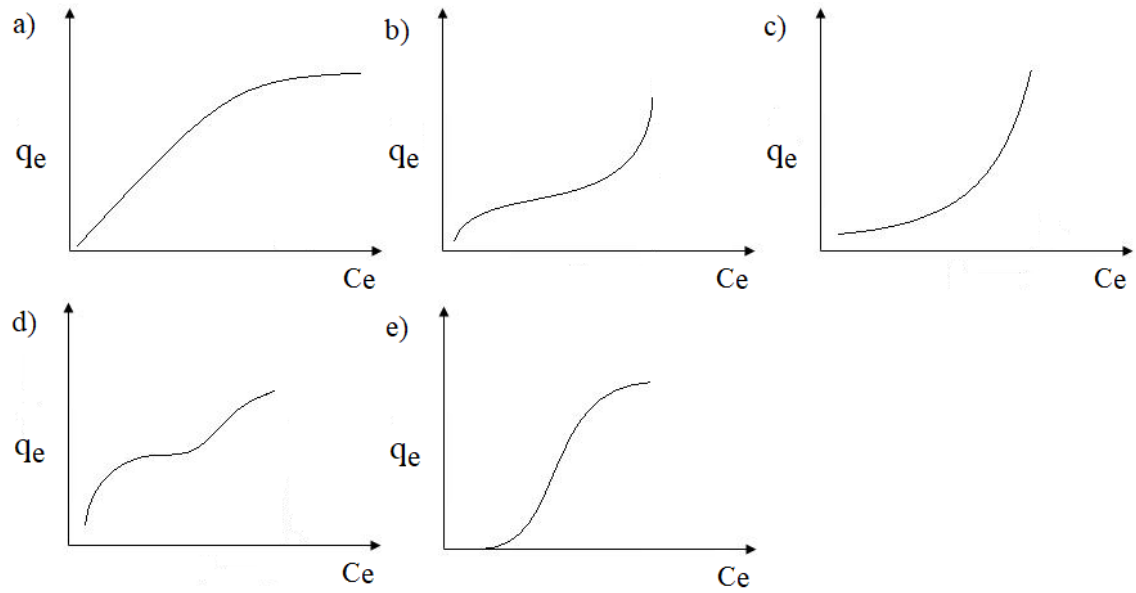

Figure 1 Types of isotherm a) type I b) type II c) type III d) type IV e) type V

Source: Khalfaoui et al.2003

Several adsorption isotherm models have been developed, and widely used, to describe adsorption monolayer formation where the temperature is fixed. Langnuir isotherm model assumes a complete monolayer coverage of the solid adsorbent

(Langmuir, 1916) and is given by equation 1, where q_e (mg g^{-1}) is the equilibrium adsorption capacity, q_{max} (mg g^{-1}) is the maximum adsorption capacity corresponding to complete coverage of available sites, C_e (mg L^{-1}) the equilibrium concentration of metal ions in solution, k_L (L mg^{-1}) is the Langmuir isotherm constant.

$$q_e = \frac{q_{max} k_L C_e}{1 + k_L C_e} \qquad \textit{Eq. 1}$$

Equation 1 can be rearranged to the linear form expressed in equation 2.

$$\frac{C_e}{q_e} = \frac{1}{k_L q_{max}} + \frac{C_e}{q_{max}} \qquad \textit{Eq. 2}$$

The Freundlich isotherm is an empirical equation which takes into account heterogeneous adsorption (Freundlich, 1906). The Freundlich isotherm equation is described in equation 3 where q_e (mg g^{-1}) is the equilibrium adsorption capacity, C_e (mg L^{-1}) is the equilibrium concentration, k_F is the Freundlich constant which is the relative adsorption capacity of the adsorbent, n is the Freundlich constant which indicates adsorption intensity. If *1/n* is closer to 1 the adsorption is more homogeneous and if *1/n* is closer to 0 the adsorption is more heterogeneous.

$$q_e = k_F . C_e^{\frac{1}{n}} \qquad \textit{Eq. 3}$$

Equation 3 can be rearranged to the linear form expressed in equation 4. The isotherm can be obtained by plotting *log* q_e against *log* C_e.

$$\log q_e = \log k_F + \frac{1}{n} \log C_e \qquad \textit{Eq. 4}$$

Extended Langmuir model is used to analyse the isotherm of the multicomponent system. This model takes into consideration the competitive forces that occur during adsorption (Singh et al. 2017). Equation 5 shows the general form of this equation which can model a system with several components.

$$q_{e,i} = \left(q_{max} k_{L,i} C_{e,i}\right) / \left(1 + \sum_{j=1}^{N} k_{L,j} C_{e,j}\right) \qquad \textit{Eq. 5}$$

As the system being studied contains only nickel and zinc equation 5 can be used to deduced equation 6 and equation 7 which can be used to analyse the nickel component and the zinc component of the binary system respectively where $q_{e,Ni}$ (mg g^{-1}) is the equilibrium adsorption capacity of nickel at equilibrium, $C_{e,Ni}$ (mg L^{-1}) is the equilibrium concentration of nickel, $k_{L,Ni}$ (L mg^{-1}) is the Langmuir constant for nickel, $q_{e,Zn}$ (mg g^{-1}) is equilibrium adsorption capacity of zinc at equilibrium, $C_{e,Zn}$ (mg L^{-1}) is the equilibrium concentration of zinc, $k_{L,Zn}$ (L mg^{-1}) is the Langmuir constant for zinc, and q_{max} (mg g^{-1}) is the maximum capacity for the binary system.

$$\boldsymbol{q_{e,Ni} = \frac{(q_{max} k_{L,Ni} C_{e,Ni})}{(1 + k_{L,Ni} C_{e,Ni} + k_{L,Zn} C_{e,Zn})}} \qquad \textit{Eq. 6}$$

$$\boldsymbol{q_{e,Zn} = \frac{(q_{max} k_{L,Zn} C_{e,Zn})}{(1 + k_{L,Ni} C_{e,Ni} + k_{L,Zn} C_{e,Zn})}} \qquad \textit{Eq. 7}$$

2.5 Kinetic models and thermodynamic analysis

Kinetics is the study of how the reaction takes place over time and at which rate. By studying the kinetics it is possible to find out the how different conditions such as temperature or pH affect the mechanism of adsorption, the amount of adsorption overtime and the rate at which it occurs. It would be essential when trying to determine how long to carry out the adsorption as well as what conditions would be ideal for the system to be the most efficient.

Lagergren pseudo-first model has been used by many researches to study adsorption where the sorbate interaction was not significant, and usually modelled accurately only the initial adsorption (Kumar. 2005). The pseudo-second order model was shown to be accurate in modelling the whole adsorption process.

Lagergren pseudo first order which was proposed by Lageregen (1898) describes physisorption and can be derived from the integrated rate law (equation 8) where k_1 (min^{-1}) is the rate constant of first order sorption, q_e (mg g^{-1}) is the amount of solute adsorbed at equilibrium, q_t (mg g^{-1}) is amount of solute adsorbed on the surface of the sorbent at any time t.

$$\frac{dq_t}{dt} = k_1(q_e - q_t) \qquad \textit{Eq. 8}$$

Equation 8 can be rearranged to a linearized form which is more commonly used. *Log(q_e)* and k_1 (min^{-1}) can be determined from the intercept and slope of the plot of *log(q_e-q_t)* against *t* (min) as shown in equation 9.

$$log(q_e - q_t) = log(q_e) - \frac{k_1}{2.303}t \qquad \textit{Eq. 9}$$

Lagergren pseudo second order model was proposed by Ho (1995) and can be used to study processes where the adsorption reaction is the rate determining step. The solute and the adsorbent undergo a chemical reaction i.e. chemisorptions takes place. Lagergren pseudo second order can be derived from the integrated rate law (equation 10) where k_2 (g mg^{-1} min^{-1}) is the rate constant of adsorption, q_e (mg g^{-1}) the amount of divalent metal ions adsorbed at equilibrium, and q_t (mg g^{-1}) is the amount of divalent metal ions on the surface of the adsorbent at time, *t* (min).

$$\frac{dq_t}{dt} = k_2(q_e - q_t)^2 \qquad \textit{Eq. 10}$$

The integrated form of equation 10 can be rearranged to its linear for equation 11. The values of k_2 (g mg^{-1} min^{-1}) and q_e (mg g^{-1}) can be determined from the intercept and slope from the plot of $\frac{t}{q_t}$ (min g mg^{-1}) against *t* (min).

$$\frac{t}{q_t} = \frac{1}{k_2 {q_e}^2} + \frac{1}{q_e}t \qquad \textit{Eq. 11}$$

The initial adsorption rate (Kalavanty et al. 2005) can be calculated using equation 12 where k_2 (g mg^{-1} min^{-1}) is the rate constant of adsorption, q_e (mg g^{-1}) the amount of divalent metal ions adsorbed at equilibrium.

$$h = k_2 {q_e}^2 \qquad \textit{Eq. 12}$$

However in instances where this equation cannot be used, such as when there is a considerable amount of desorption after the initial adsorption, the experimental initial adsorption rate, h_{exp} can be estimated using equation 12 with the values of k_2 and q_e calculated using only the data during the initial adsorption.

Intraparticle diffusion model (Cheung et al. 2007) was used to analyse the adsorption involves the transportation of the solute from the aqueous phase to the solid surface and then a diffusion of the solute into the pores of the solid. This is described by equation 13 where q_t (mg g^{-1}) is the amount adsorbed at time t (min). The rate constant k_{id} (mg $g^{-1}min^{-1/2}$) is directly evaluated from the slope of the regression line. The intercept c (mg g^{-1}) provides information of the thickness of the boundary layer, the larger the intercept the larger the boundary effect.

$$q_t = k_{id}.t^{\frac{1}{2}} + c \qquad \textit{Eq. 13}$$

Based on the shape of the intraparticle diffusion graph and the way the regression lines intercept qualitative information about the mechanism of adsorption can be deduced as shown in Figure 2. In a two step in the adsorption process there is external mass transfer followed by intraparticle diffusion. If there are three intercepting lines of regression it can be deduced that after external mass transfer there are two distinct intraparticle diffusion steps; macropore diffusion followed by micropore diffusion. If there is a regression line which has a negative slope it indicates that desorption is occurs as the system reaches equilibrium. Desorption can occur after the intraparticle diffusion step or in some cases after the external mass transfer step, in that case it indicates there is no intraparticle diffusion or that it is not significant compared to the amount of desorption.

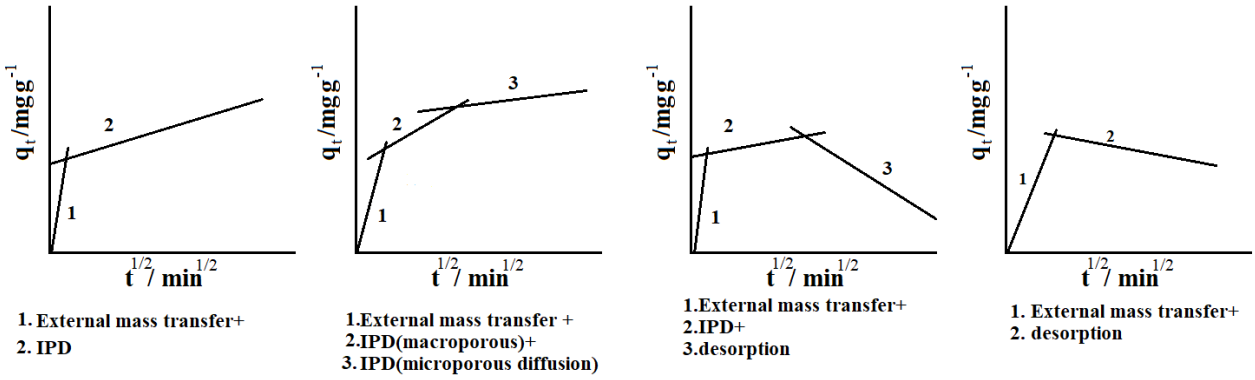

Figure 2 Explanation for the shapes of the plot of the intraparticle diffusion model

Thermodynamics study of adsorption can be used to determine how spontaneous a reaction is under certain conditions as well as the entropic and enthalpy driving forces of the reaction process.

The thermodynamic potential of the adsorption systems at four different temperatures were determined using the value of k_d (L g^{-1}) calculated using equation 14 and then substituted into equation 15 to calculate ΔG^o (J mol^{-1}) which is the change in free energy, R is the gas constant (8.314 J mol^{-1} K^{-1})and T is the temperature (K) (Sharifipour et al. 2015) The standard enthalpy ΔH^o and the standard entropy ΔS^o were determined from the Van Hoff's equation (16).

$$\boldsymbol{k_d = \frac{q_e}{C_e}} \qquad \textit{Eq. 14}$$

$$\boldsymbol{\Delta G^o = -RTlnk_d} \qquad \textit{Eq. 15}$$

$$\boldsymbol{lnk = \frac{\Delta S^o}{R} - \frac{\Delta H^o}{RT}} \qquad \textit{Eq. 16}$$

2.6 Summary

The literature review highlights that it is important to develop a system to remove dangerous pollutants from water in developing countries,which is efficient, simple to carry out and affordable at both large and small scales. Adsorption is seen as a viable method due to its ease of application. The main cost in this process is the adsorbent. Hence the chosen adsorbent to be used in developing countries should ideally be affordable, readily available and environmentally friendly. For a tropical country like Sri Lanka bio-waste such as tea waste, rice husks and coir pith are ideal sources of adsorbent to be used.

CHAPTER 3: RESEARCH METHODOLOGY

3.1 General

This chapter describes the methodology followed for the research study. It includes the selection, characterization, and determination of the particle density of the adsorbent, preparation of stock solutions for batch adsorption test, determination of the adsorption isotherms, and study of the effect of pH on the adsorption of metal ions onto adsorbent, and adsorption kinetics of metal ion onto adsorbent.

Based on literature reviewed in the previous chapter (Amarasinghe, 2007, 2011), low cost and the availability, coir pith was chosen as the adsorbent for this study. Coir pith is made up of mostly lignin and cellulose, which are organic polymers containing many polar surface functional groups such as esters, ethers and carbonyl groups. Nickel and Zinc were selected as heavy metals considering the heavy use of the materials in industries as described in the previous Chapter.

3.2 Preparation of the Adsorbent

Coir pith was obtained from Sampath Coir Mill, Singakkuliya, Sri Lanka and dried in the oven using stainless steel trays at 60 °C for 12 hours. It was sieved using a sieve shaker to obtain particles with a size distribution between 335 μm and 1 mm. The coir pith was washed with distilled water and then dried in the oven at 60 °C for 12 hours.

3.3 Characterization of the Adsorbent

To determine the surface functional groups Fourier transform infrared spectrometer (FTIR) analysis of coir pith before adsorption, after nickel adsorption, after zinc adsorption and binary adsorption was carried out. The position and intensity of the peaks of the in the infrared spectrometer analysis allowed the functional groups to be identified as well as how the adsorption effected the prevalence and strength of these functional groups. Coir pith before adsorption was imaged using scanning electron microscopy (SEM) at 500x magnification to determine the pore structure and size.

3.4 Determination of particle density of Coir Pith Adsorbent

Particle density was determined using the specific gravity bottle method. A washed and oven dried 50 ml specific gravity bottle was weighed (W1) and then around 1.5 g of coir pith was added and then weighed again (W2). Enough coconut oil to cover the coir pith was added and was allowed time to soak completely. More coconut oil was then added to fill the bottle completely and then weighed again (W3). The bottle was then emptied, cleaned and oven dried and filled with oil completely and then weighed again (W4). The bottle was emptied, washed, dried, filled with distilled water, and then weighed (W5).

Particle density, ρ_{true} (g cm^{-3}), was calculated using the equation 17.

$$\boldsymbol{\rho_{true}} = \frac{(\boldsymbol{W2} - \boldsymbol{W1})(\boldsymbol{W4} - \boldsymbol{W1})}{(\boldsymbol{W5} - \boldsymbol{W1})((\boldsymbol{W4} - \boldsymbol{W1}) - (\boldsymbol{W3} - \boldsymbol{W2}))} \qquad \textit{Eq. 17}$$

Bulk density was measured using a weighed 10 cm^3 measuring cylinder filled with coir pith and then compressed until it filled the cylinder. Weight was measured and the volume, according to the reading on the measuring cylinder, of the coir pith was noted. The bulk density, ρ_{bulk} (g cm^{-3}) was calculated using the equation 18 where $V_{coirpith}$ is the volume of coir pith and $m_{coirpith}$ is the mass of coir pith.

$$\boldsymbol{\rho_{bulk}} = \frac{\boldsymbol{V_{coirpith}}}{\boldsymbol{m_{coirpith}}} \qquad \textit{Eq. 18}$$

Porosity, φ, was determined using equation 19 where ρ_{bulk} (g cm^{-3}) is bulk density and ρ_{true} (g cm^{-3}) is particle density.

$$\boldsymbol{\varphi} = \mathbf{1} - \frac{\boldsymbol{\rho_{bulk}}}{\boldsymbol{\rho_{true}}} \qquad \textit{Eq. 19}$$

3.5 Preparation of stock solutions for batch adsorption test

The stock solution of 1000 mg L^{-1} Ni(II) and Zn(II) were prepared from analytical grade nickel nitrate $Ni(NO_3)_2.6H_2O$ and zinc nitrate $Zn(NO_3)_2.6H_2O$ (supplied by Sigma-Aldrich chemicals, Germany). 4.95 g of nickel nitrate hexahydrate was dissolved in 1000 ml of distilled water using a 1000 ml volumetric flask to prepare a solution of with a Ni(II) concentration of 1000 mg/L. 3.60 g of zinc nitrate hexahydrate was dissolved in 1 L of distilled water using a 1 L volumetric flask to

prepare a solution of with a Zn(II) concentration of 1000 mg/L. Refer Appendix for calculations.

3.6 Effect of dose of coir pith on metal ion adsorption

Synthetic waste water with volume 500 cm^3 of nickel solution with concentration 25 mg L^{-1} was made up by diluting 12.5 cm^3 of the stock solution with concentration 1000 mgL^{-1} with 487.5 cm^3 of distilled water. Coir pith of mass 0.125 g, 0.25 g, 0.5 g. 1 g and 2 g were each added to identical beakers with 500 ml solution and the mixtures were stirred using an agitator at 30 ^oC. After 120 minutes when the solution has reached equilibrium the 50 cm^3 samples of the solution were filtered using a filter paper and analysed using inductively coupled plasma mass spectrometry (ICP-MS) to determine the final concentration.

3.7 Determination of the adsorption isotherms

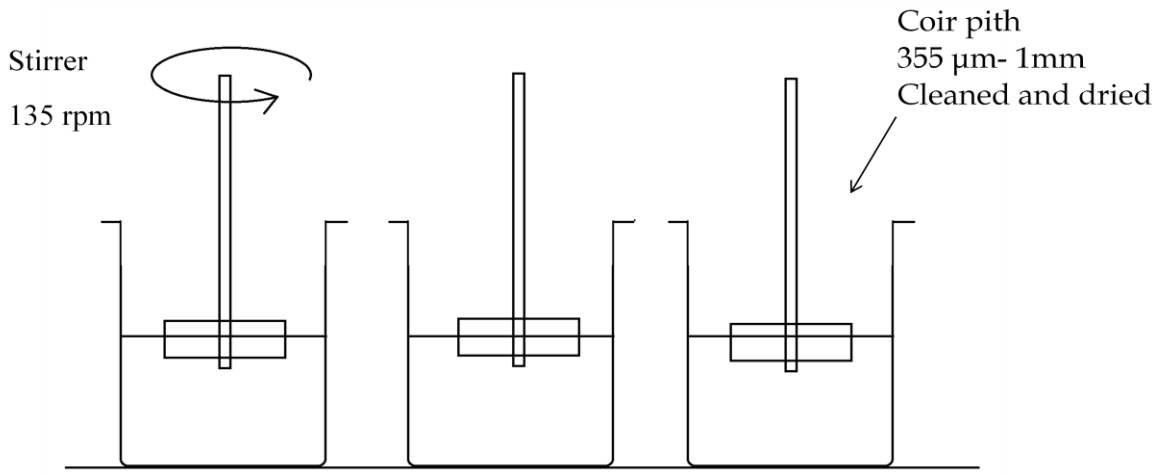

Figure 3 Batch experiment set up for the Isotherm study

3.7.1 Adsorption isotherm of single system adsorption onto coir pith

500 cm^3 solutions with initial concentrations of 10 mg L^{-1}, 20 mg L^{-1}, 50 mg L^{-1}, 100 mg L^{-1} and 200 mg L^{-1} (refer Appendix for details) were made by diluting stock solutions of concentration 1000 mg L^{-1} using distilled water. 0.75 g of the coir pith adsorbent was added to the solution and stirred using an agitator system at a speed of

135 rpm at 30 °C (Figure 3). After 120 minutes when the solution has reached equilibrium the 50 cm^3 samples of the solution were filtered using a filter paper and analysed using inductively coupled plasma mass spectrometry (ICP-MS) to determine the final concentration.

3.7.2 Adsorption isotherm of binary adsorption onto coir pith

500 cm^3 solutions of nickel and zinc with a 1:1 ration and a combined initial concentrations of 10 mg L^{-1}, 20 mg L^{-1}, 50 mg L^{-1}, 100 mg L^{-1} and 200 mg L^{-1} (refer Appendix for details) were made by diluting stock solutions of concentrations 1000 mg L^{-1} using distilled water. 0.75 g of the coir pith adsorbent was added to the solution and stirred using an agitator system at a speed of 135 rpm at 30 °C. After 120 minutes when the solution has reached equilibrium the 50 cm^3 samples of the solution were filtered using a filter paper and analysed using inductively coupled plasma mass spectrometry (ICP-MS) to determine the final concentration.

3.8 Study of the effect of pH on the adsorption of metal ions onto coir pith

3.8.1 Effect of pH on single system adsorption of nickel or zinc onto coir pith

500 cm^3 solutions with metal ion concentration 50 mgL^{-1} was made by diluting 25 cm^3 of stock solutions of concentration 1000 mg L^{-1} using 475 cm^3 distilled water. The pH was adjusted using 0.5 M solution of sulphuric acid (H_2SO_4) to obtain solutions of pH 3, pH 4, and pH5. A solution of pH 8 was obtained using 0.1 M solution of sodium hydroxide (NaOH) in addition to a solution with pH 7 which was not adjusted by either acid or base. The modification in pH was monitored using a pH meter. 0.75 g of the coir pith adsorbent was added to each metal ion solution and stirred using an agitator system at a speed of 135 rpm at 30 °C for 1 hour (Figure 3). 50 cm^3 samples of the solution were filtered using a filter paper and analysed using inductively coupled plasma mass spectrometry (ICP-MS) to determine the final concentration.

3.8.2 Effect of pH on binary adsorption of nickel and zinc onto coir pith

500 cm^3 solutions with nickel and zinc in a 1:1 ratio with a combined concentration 50 mgL^{-1} was made by diluting 12.5 cm^3 of stock solutions of concentration 1000 mg L^{-1} using 475 cm^3 distilled water. The pH was adjusted using 0.5 M solution of sulphuric acid (H_2SO_4) to obtain solutions of pH 3, pH 4, and pH5. A solution of pH 8 was obtained using 0.1 M solution of sodium hydroxide (NaOH) in addition to a solution with pH 7 which was not adjusted by either acid or base. The modification in pH was monitored using a pH meter. 0.75 g of the coir pith adsorbent was added to each metal ion solution and stirred using an agitator system at a speed of 135 rpm at 30 °C for 1 hour. 50 cm^3 samples of the solution were filtered using a filter paper and analysed using inductively coupled plasma mass spectrometry (ICP-MS) to determine the final concentration.

3.9 Study of the kinetics of metal ion adsorption onto coir pith

The kinetic study was carried out at temperatures of 30 °C, 40 °C, 50 °C and 60 °C using the same initial solution concentration, volume, mass of coir pith adsorbent and conditions varying only the temperature and the time at which samples were taken. Identical reaction mixtures were carried out with samples taken out at different times. The temperature was kept constant using a water bath. The solutions were allowed to reach their target temperature before coir pith was added.

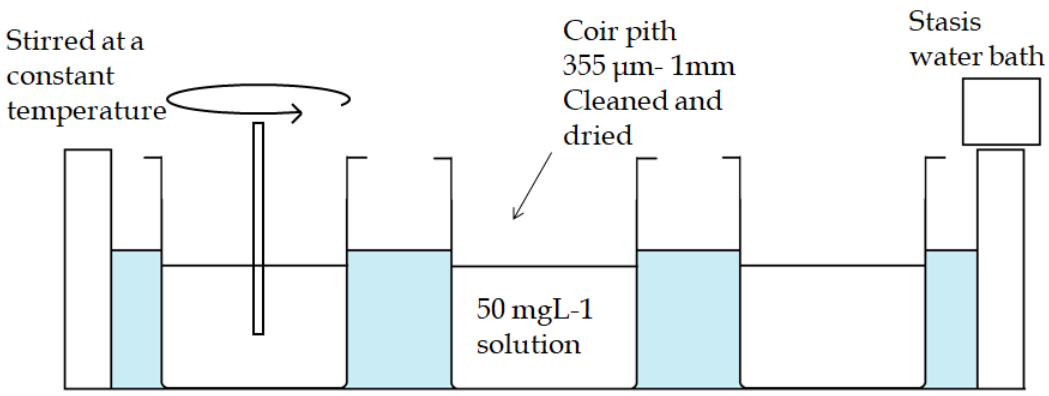

Figure 4:Batch experiment set up for kinetic study

3.9.1 Study of adsorption kinetics of nickel or zinc ion adsorption onto coir pith

For the single system studies 500 cm^3 solution of synthetic waste water with metal ion concentration 50 mg L^{-1} was made up by diluting 25 cm^3 of either nickel or zinc stock solution of concentration 1000 mg L^{-1} with 475 cm^3 of distilled water. The solution was allowed to reach the target temperature in the stasis water bath before 0.75 g of coir pith was added. The solution mixture was stirred using a clean spatula as shown in figure 5. Samples were taken out at 1 minutes, 2 minutes, 5 minutes, 10 minutes and 30 minutes. 50 cm^3 samples of the solution were filtered using a filter paper and analysed using inductively coupled plasma mass spectrometry (ICP-MS) to determine the final concentration.

For the binary system study 500 cm^3 solution of total metal ion concentration 50 mg L^{-1} was made up by diluting 12.5 cm^3 of each nickel and zinc stock solution of concentration 1000mg L^{-1} with 475 cm^3 of distilled water. The rest of identical to the single system study.

3.9.2 Analysis of the kinetic data

The kinetic data was analysed using the Lagergren pseudo first order equation and Lagergren pseudo second order reaction models to study the rate and mechanism of adsorption. Depending on the data it was analysed using either the graphical method which involved plotting the data on a graph according to the models or by using the data fitting method.

For example when using the data fitting method with the Lagergren pseudo second order model was used to determine the values of rate constant k^2 (g $mg^{-1}min^{-1}$) and equilibrium adsorption capacity q_e (mg g^{-1}). While for the graphical method the linear form of the model was used to plot a straight line, for the data fitting method the non-linear form of equation 11 was used as shown in equation 20.

$$q_t = \frac{q_e^2 k_2 t}{1 + k_2 q_e t} \qquad \textit{Eq. 20}$$

First the values of q_e and k_2 were approximated and then substituted in the equation to derive approximate values of q_t. The experimental values of q_t were subtracted by the predicted values of q_t and then squared to get R^2 value for each time. The sum of the R^2 values were determined and then using the solver function in excel the sum of the R^2 values were set to find the possible minimum value of the sum of R^2 by changing the values of q_e and k_2. The new values of q_e and k_2 output by solver should be most accurate values of q_e and k_2 for the model to match the experimental data.

CHAPTER 4: RESULTS AND DISCUSSION

4.1 Overview

The coir pith adsorbent as well as the single and binary adsorption process of nickel and zinc onto coir pith under various conditions was studied. The effect of pH, temperature, dose and adsorption over time were studied in order to understand the mechanism of adsorption, the nature of the adsorption and how to optimise the adsorption process. Results obtained are presented and discussed in this section.

4.2 Characterization of adsorbent by Scanning ElectronMicroscopy (SEM)

The surface morphology of coir pith adsorbent was examined by scanning electron microscopy (SEM) and is shown in Figure 5 Coir pith is a low density adsorbent with pores of various sizes with diameters between 25 to 50 µm. The low density and porous structure of coir pith allows a large surface of the adsorption of heavy metals. The structures of the coir pith are long channels arranged in a honey comb structure. The surface of the coir pith is also rough with micro pores which offer an excellent surface for molecular adhesion.

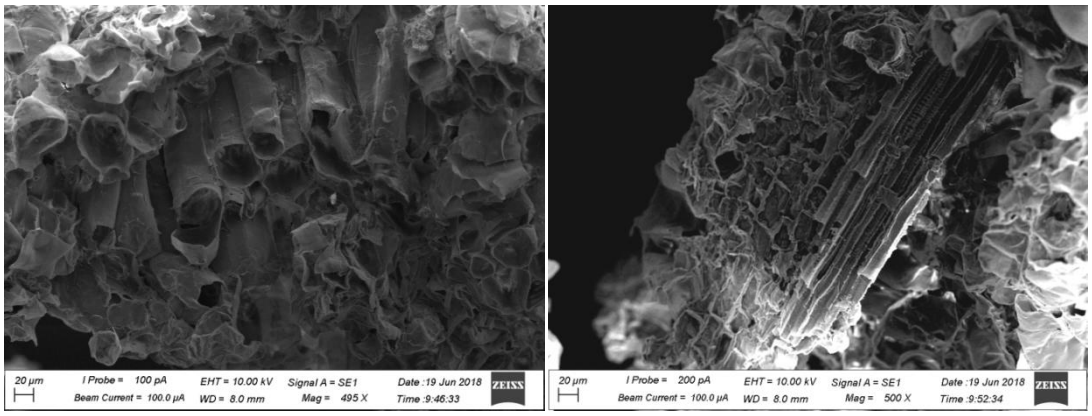

Figure 5 Scanning electron microscopy image of the surface of coir pith before adsorption at a magnification of 500 times, a) mouths of the pores of coir pith, b) exposed channels of the coir pith pores

4.3 Particle size distribution and density determination

The particle size distribution was determined using sieve analysis as shown in *Figure 6* in the range between 1000 µm and 335 µm . The average particle size was determined to be 686 µm. 47% of the coir pith was within the range 1000-710 µm, 34 % of the coir pith was within the range 710- 500 µm and 19 % of the coir pith was within the range of 500- 335 µm.

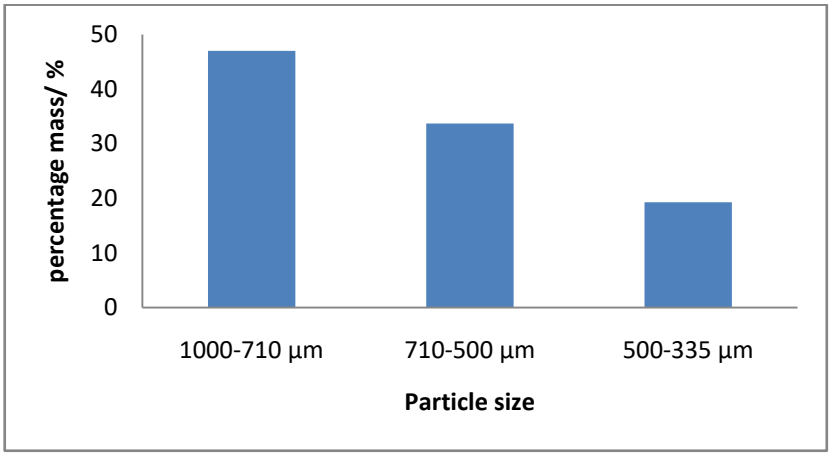

Figure 6. Particle size of coir pith against percentage mass of coir pith

The particle density was determined using the specific gravity bottle method with oil as the medium and the true density (ρ_{true}) calculated using equation 17 was found to be 0. 497 gcm^{-3}. This was less than typically found in the literature. In a study about the physical properties of coir pith by Neethi et al. (2006) found the density value to be between 0.939 – 0. 605 g cm^{-3}, however this was at a variety of moisture content and a slightly different particle size range which could have lead to this discrepancy.

In a different study by Amarsinghe (2007) the particle density was found to be 0.799 g cm^{-3} when using oil and a measuring cylinder to determine volume. This difference might be due to the difference in type of coconut, the dryness, age, and particle size of the coir pith. The bulk density (ρ_{bulk}) calculated using equation 18 was found experimentally to be 0. 114 g cm^{-3} which was within range of the bulk density found by Neethi et al. (2006) which was 0.097- 0.341 gcm^{-3} and Amarasinghe (2007) 0.116 g cm^{-3}. From the experimentally determined values of particle density and bulk density the porosity was calculated and found to be 0.77.

4.4 Effect of dose of coir pith adsorbent and the initial heavy metal concentration on the adsorption of nickel metal ions

The effect of adsorbent dose was studied by finding the percentage of metal ions removed as shown in Figure 7 and the equilibrium adsorption capacity as shown in Figure 8, when different amounts of adsorbent with nickel solutions of concentration 25 mg L^{-1} at 30 °C.

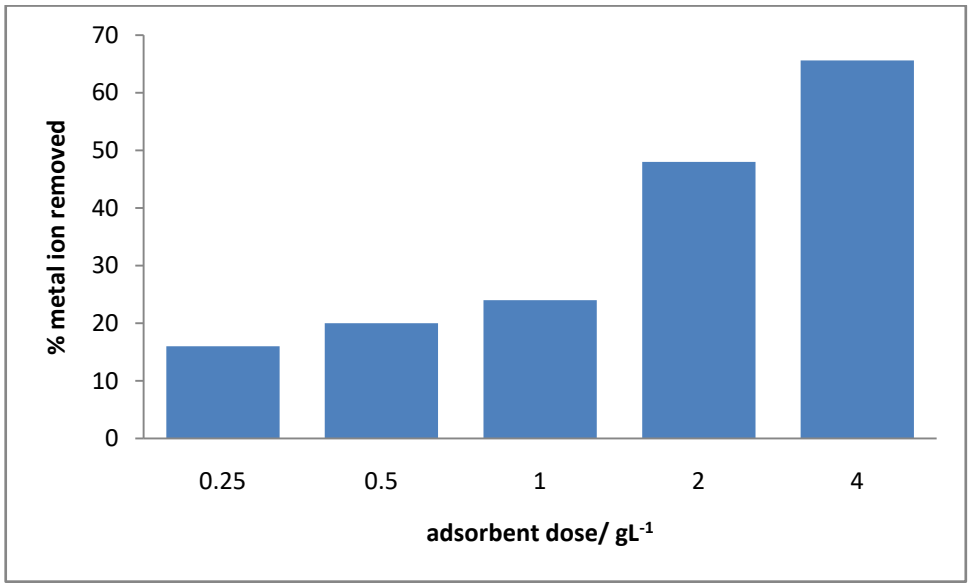

Figure 7. Percentage of nickel metal ion removed at equilibrium against coir pith adsorbent dose for a solution with an initial concentration of 25 mgL^{-1} at 30 °C

The adsorption of nickel increases with the increase in dosage of adsorbent due to the increase in the surface for adsorption to occur.

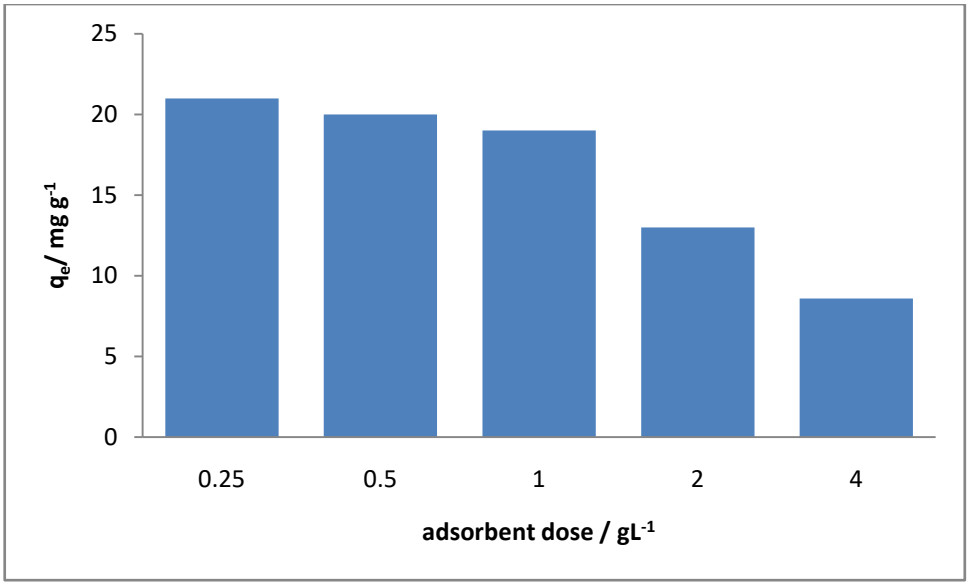

Figure 8.Equilibrium adsorption capacity of nickel ions against coir pith adsorbent dose for a solution of initial concentration 25 mgL^{-1} at 30 °C

The equilibrium adsorption capacity decreases with increase in dosage of adsorbent despite more adsorption occurring overall as the increase in adsorption is less than proportional to the increase in the amount of adsorbent. This is likely because as there is more adsorption the concentration gradient decreases and the driving force for adsorption decreases.

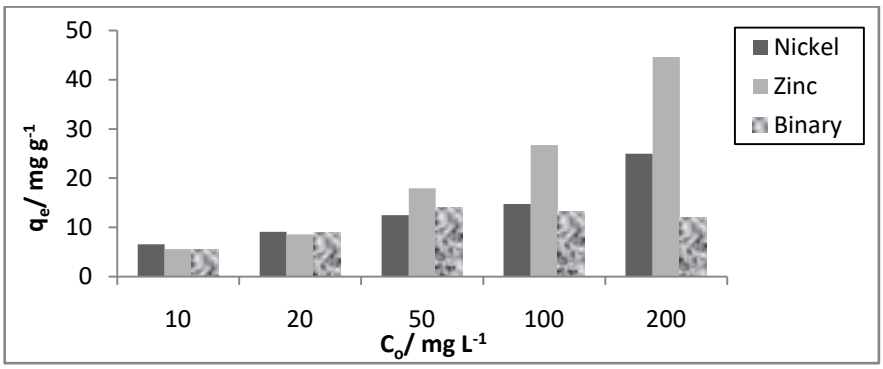

Figure 9.Equilibrium adsorption capacity against initial concentration for the single and binary systems of nickel and zinc

From figure 9 it is evident that at low initial metal ion concentrations the amount of adsorption is roughly equal in all three systems however at higher concentrations the amount of zinc adsorption is much greater than that for nickel or in the binary

system. This suggests the initial concentration has a large effect on the amount of zinc as the concentration gradient being a primary driving force for the adsorption. At higher initial concentrations in the binary system the adsorption capacity stops increasing with increase in initial concentration suggesting that the surface becomes saturated and no further adsorption can occur. This is not observed in the single system adsorption for either nickel or zinc under the range of concentration studied. This suggests the competitive environment of the binary adsorption system limits the adsorption or effects the mechanism or degree to which adsorption occurs.

4.5 Adsorption isotherms for nickel, zinc and the binary system

The adsorption isotherm gives information about the mechanism of metal ions adsorbs on the adsorbent surface. It was constructed by plotting a graph of equilibrium adsorption capacity, q_e(mg g^{-1}), against equilibrium concentration, C_e (mg L^{-1}) at a constant temperature of 30 ^{o}C for solutions of various initial concentrations to which 0.75 g of coir pith adsorbent had been added. By studying the difference in adsorption equilibrium over a range of concentrations it is possible to determine the maximum adsorption capacity of the adsorbent. Figure 10 shows the plot of q_e (mgg^{-1}) against C_e (mgL^{-1}) for the adsorption of single system nickel, single system zinc, and binary system adsorption.

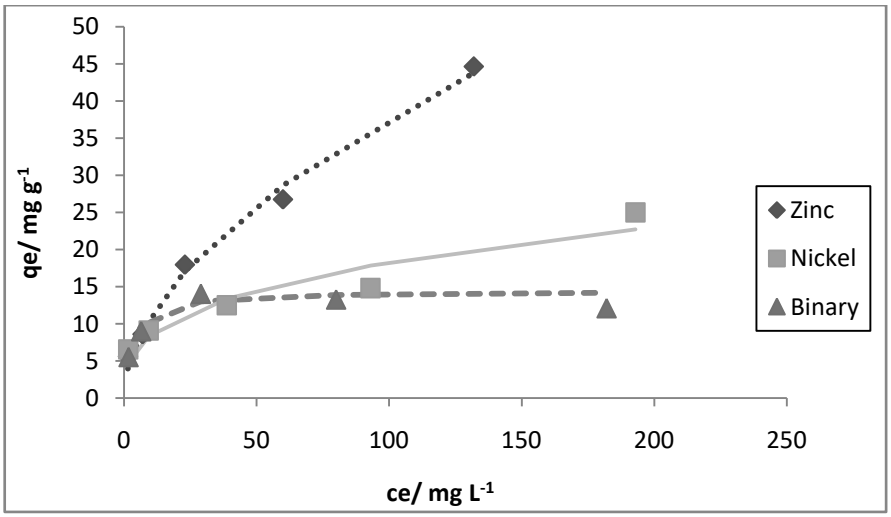

Figure 10. Adsorption isotherms of single system zinc, single system nickel and the binary system of equilibrium adsorption capacity against equilibrium concentration at 30 ^{o}C

The regression line for the single system isotherms was drawn using the Freundlich constants shown in Table 5. The regression line for the binary system was drawn using the calculated Langmuir values shown in Table 5. The adsorption capacity of coir pith for zinc is much higher than that for nickel or the binary system. In the range of concentrations tested, the coir pith had not reached full saturation for either nickel or zinc but had reached full saturation for the binary system by an initial metal ion concentration of 50 mg L^{-1}. As the binary system has an adsorption capacity less than the average of the single system adsorptions we can infer that the binary environment interferes with the adsorption process.

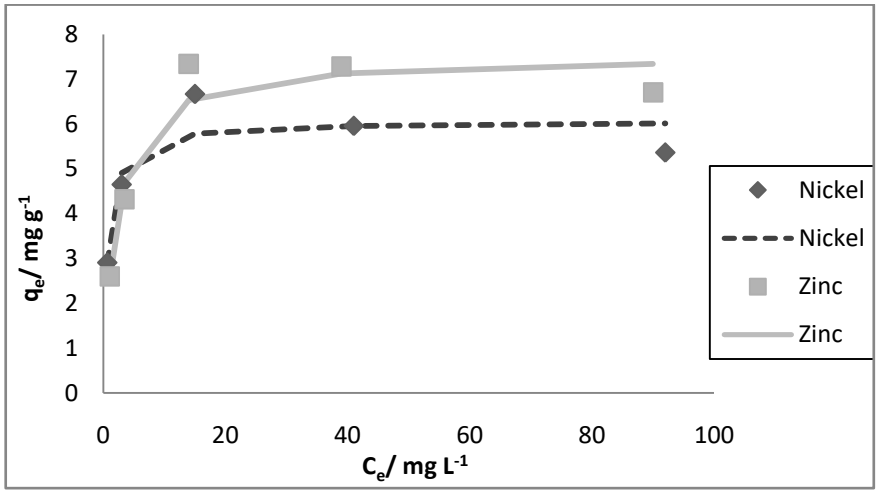

Figure 11. Adsorption isotherms of the nickel and zinc components of the binary system of 30 °C

Figure 11.which shows the nickel and zinc components of the binary system at 30 °C show the amount of zinc adsorbed is more than the amount of nickel adsorbed, which is similar to the behaviour of the single system where there is more zinc adsorption than nickel adsorption. The disparity between the two amounts however is much less compared to their equivalents in the single system.

The competitive behaviour was studied using the ratios between the equilibrium adsorption capacity of a metal in the binary system (q_e) and the equilibrium adsorption capacity of the single system for that metal (q_m). The q_e values are doubled as the initial concentration of the metal ions component is half that of the

metal ion in the binary system. When the ratio of q_e/q_m is greater than 1 it means the adsorption is promoted and therefore the presents of other metals would result in synergism, if q_e/q_m is equal to 1 there is no interaction between the metal ions, and if the ratio of q_e/q_m is less than 1 the metal ions are antagonistic.

If metal ions are synergistic the adsorption is promoted and the different metal ions have different adsorption sites while if the metal ions are antagonistic the metal ions compete over the same adsorption sites. Figure12 shows how the ratio changes as the concentration changes. At lower concentrations there is no competition between the metal ions.

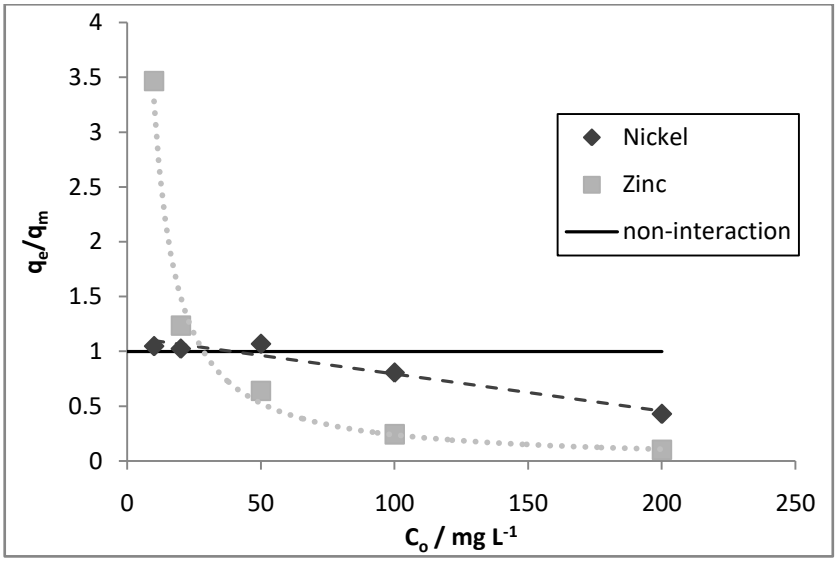

Figure 12.Equilibrium adsorption capacity ratios q_e/q_m against initial concentration of the metal ions.

For nickel the equilibrium adsorption capacity ratios is approximately one until the concentration is increased above 50 mg L^{-1}, after which the ratio decreases suggesting at higher concentrations nickel and zinc become more antagonistic. Zinc is shown to have synergistic behaviour at lower concentrations with the ratio being greater than 1, however like for nickel at higher concentrations the ratio becomes less than 1 due competition. When comparing Figure 12 with Figure 10 and Figure 11 it is evident that when the initial solution concentration above 50 mg L^{-1} the

adsorbent surface becomes saturated resulting in an decrease in equilibrium adsorption ratio.

The data from the nickel and zinc single system adsorption at 30 °C was fitted to the Lagmuir and Freundlich isotherm models. The Langmuir parameters q_{max} (mg g^{-1}) and k_L (Lm g^{-1}) were calculated using equation 2 and the Freundlich parameters k_F and 1/n were calculated using equation 4 and the results are shown in *Table 5*.

Table 5 Isotherm parameters for the single system and binary adsorption of nickel and zinc solutions onto 0.75 of coir pith at 30 °C

Type of isotherm	Single system		Binary system		
Parameter	Ni	Zn	Ni	Zn	Combined
Langmuir	$q_e = \frac{q_{max} K_L C_e}{1 + K_L C_e}$				
q_{max} (mg g^{-1})	23.23	65.04			14.4
k_L (L mg^{-1})	0.045	0.014			0.32
R^2	0.89	0.96			0.99
Freundlich	$q_e = K_F C_e^{\frac{1}{n}}$				
k_F	3.99	3.17			6.95
1/n	0.33	0.53			0.13
R^2	0.98	0.97			0.57
Competitive Langmuir	$q_{e,i} = \frac{q_{max} . k_{L,i} . C_{e,i}}{1 + k_{L,i} . C_{e,i} + k_{L,j} . C_{e,j}}$				
q_{max} (mg g^{-1})					13.6
k_L (L mg^{-1})			0.30	0.35	
R^2			0.50	0.54	
Non-competitive Langmuir	$q_{e,i} = q_{max} (\frac{k_{L,i} . C_{e,i} + k_{L,i,j} . C_{e,i} . C_{e,j}}{1 + k_{L,i} . C_{e,i} + k_{L,j} . C_{e,j} + k_{L,i,j} . C_{e,i} . C_{e,j}})$				
q_{max} (mg g^{-1})					6.65
k_L (L mg^{-1})			0.73	0.48	0.64
R^2			0.69	0.62	

Modified Competitive Langmuir model	$q_{e,i} = \frac{q_{max\,,i}.k_{L,i}.C_{e,i}}{1 + k_{L,i}.C_{e,i} + k_{L,j}.C_{e,j}}$				
q_{max}(mg g^{-1})			99.3	7.51	
k_L(L mg^{-1})			0.05	0.75	
R^2			0.51	0.51	
Langmuir-Freundlich	$q_{e,i} = \frac{q_{max}.k_{LF,i}.(C_{e,i})^{\frac{1}{n,i}}}{1 + k_{LF,i}.(C_{e,i})^{\frac{1}{n,i}} + k_{LF,j}(C_{e,j})^{\frac{1}{n,j}}}$				
q_{max}(mg g^{-1})			13.44		
k_{LF}			0.46	0.32	
1/n			0.93	1.09	
R^2			0.89	0.83	

The Langmuir parameter q_{max} (mg g^{-1}) is the maximum adsorption capacity and k_L (L mg^{-1}) is the equilibrium constant for the adsorption. The data for the single system nickel adsorption fit into the Langmuir model with a R^2 value of 0.89, maximum adsorption capacity, q_{max}, of 23.23mgg^{-1}, and Langmuir constant k_L, was 0.045 L mg^{-1}. The data for the single system adsorption of zinc fit better into the Langmuir model with a R^2 value of 0.96, maximum adsorption capacity, q_{max}, of 65.04 mg g^{-1}, and Langmuir constant k_L, was 0.014 L mg^{-1}.

The maximum adsorption capacity of zinc is greater than nickel however the Langmuir constant k_L which is analogous to the equilibrium constant is larger for nickel than for zinc suggesting the equilibrium favours adsorption over desorption more in nickel than in zinc. However that maybe because under equilibrium conditions the concentration of the metal ions adsorbed on the coir pith is higher for zinc therefore desorption is more favourable than for nickel.

The Freundlich parameter, k_F, which describes relative adsorption capacity, of zinc is less than that of nickel being 3.17 and 3.99 respectively. This suggests nickel has a greater affinity for the adsorbent than zinc. The Freundlich parameter *1/n* which is the adsorption intensity is greater for zinc than for nickel being 0.53 and 0.33

respectively. As both the values are between 0 and 1 the processes are confirmed to be chemisorptions. As *1/n* of nickel is closer to 0 the curvature of the isotherm is greater and the process can be interpreted as being more heterogeneous.

In order to calculate q_{max} using the Freundlich model equation 21 suggested by Halsey (1952) must be used. The Freundlich expression is an exponential equation and therefore assumes that as the initial solution concentration increases, the concentration of the solute on the adsorbent increases. The value of k_F is larger for nickel but the value for *1/n* is larger for zinc. At a lower initial concentration the q_{max} of nickel would be higher than zinc while a larger initial concentration would show a larger q_{max} for zinc. This is illustrated in Figure 13 and in the Appendix.

$$\boldsymbol{q_{max} = k_F . C_o^{\frac{1}{n}}} \qquad \textit{Eq. 21}$$

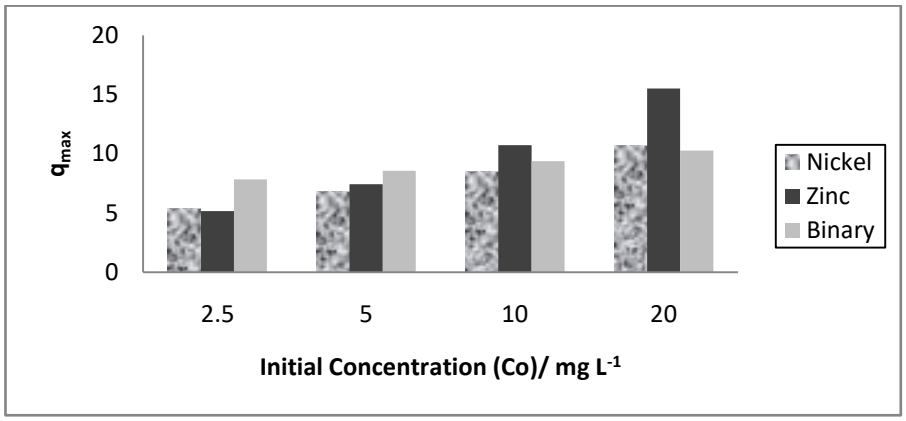

Figure 13. Initial concentration against maximum adsorption capacity (q_{max}) calculated using values derived from the Freundlich constants

The correlation coefficient R^2 for nickel and zinc for the Langmuir isotherm is less than the R^2 obtained from using the Freundlich model, thus the Freundlich model is more suitable for the analysis of this system.

The data from the binary system at 30 ^oC was fitted to the Langmuir isotherm model, and the Freundlich isotherm model, the competitive Langmuir isotherm model, non-competitive Langmuir model, modified competitive Langmuir isotherm model, the and the Langmuir-Freundlich isotherm model.

The binary system data fit into the Langmuir model well with a R^2 value of 0.99, the q_{max} value is 14.4 mg g^{-1} and the k_L value of 0.32. The q_{max} value is similar to the experimental value 14 mg g^{-1} when the adsorbent surface was saturated which was determined from the plateau of the adsorption isotherm graph Figure 10. From this it is evident that the adsorption capacity is less than the single system adsorption yet the k_L values is larger, which suggests that adsorption in the equilibrium is more favourable than in the adsorption equilibrium for the single system adsorption, probably as the binary system reaches full saturation at a lower concentration than the single systems for either metal ion. As the data fits well into this model it can be deduced that there is monolayer formation and the surface is homogenous.

When the binary data was fit into the Freundlich model and obtained a k_F value of 6.95 and a *1/n* value of 0.13. The data suggests the relative adsorption capacity of the binary system is greater than that of the single system but has lower adsorption intensity. A low *1/n* value suggests a more heterogeneous surface which contradicts what can be inferred from the graphical interpretation of the data shown in Figure 10. The low R^2 value of 0.57 shows the data does not fit the model well and cannot be used to analyse this system.

The competitive Langmuir isotherm model calculates the parameters pertaining to nickel and zinc simultaneously. This model assumes uniform surface coverage, equivalent sites and all ions compete for the same sites. The q_{max} for the whole system which includes both nickel and zinc adsorption was 13.6 mg g^{-1}, which is very similar to the value of q_{max} obtained from the Langmuir model and value of q_{max} which can be deduced from the Figure 10.

The k_L values for the nickel and zinc components were 0.30 and 0.35 respectively which is similar to the k_L value obtained when the data was fit into the Langmuir model. The k_L value for the zinc component is slightly higher than the nickel component suggesting the adsorption equilibrium of zinc is more favourable than that for nickel. This is consistent with Figure 11 which shows there is less nickel adsorption than zinc adsorption. However the R^2 value is 0.5 and 0.54 for nickel and

zinc respectively. This low correlation coefficient suggests that the competitive Langmuir model is unsuitable for this system.

The non-competitive Langmuir model assumes that the two ions can occupy the same active site simultaneously. The k_L values are 0.73 for the nickel component, 0.48 for the zinc component, and 0.64 for the whole binary system. The k_L value for the total binary system is twice that for the equivalent k_L value calculated by the Langmuir model. The q_{max} value calculated by this model is 6.65 mg g^{-1} and about half that of the previous models and the q_{max} observed in Figure 10. The correlation coefficients, R^2, are low for nickel and zinc being 0.69 and 0.62 respectively. This suggests this model is unsuitable to analyse this system and the metal ions do not occupy the same adsorption sights simultaneously.

The modified competitive Langmuir model assumes the different metals have different adsorption capacities and different adsorption sites and that the system is heterogeneous. The q_{max} values calculated by this model had a very different range than values calculated by the Langmuir model. The q_{max} value for the nickel component was 99.3 mg g^{-1} which is much larger than the q_{max} of the zinc component at 7.51 mg g^{-1} this is very dissimilar to the experimental data.

Similarly the k_L values for the nickel and zinc components are 0.05 and 0.75 respectively which suggests there is much more zinc adsorption than nickel adsorption which is inconsistent with what is observed experimentally, which is that they have roughly equal amounts of adsorption. The R^2 for nickel and zinc is 0.5, therefore this model is unsuitable to analyse this system. From this it can be deduced the binary adsorption does not behave as assumed by the model.

Langmuir-Freundlich isotherm model can describe both Langmuir type behaviour and Freundlich type behaviour, where q_{max} is the maximum adsorption capacity of the system, k_{LF} is the affinity of the adsorbent to the adsorbate and 1/n is the degree of heterogeneity. The correlation coefficient, R^2, for nickel and zinc are 0.89 and 0.83 respectively. The k_{LF} values are within a reasonable range but the k_{LF} value for nickel is 0.46 and the value for zinc is 0.32 which suggests nickel has a higher affinity for the surface than zinc, which contradicts the results shown in Figure 11.

The 1/n values for both nickel and zinc are close to 1, which suggests the surface is homogenous.

This means the surface has a uniform monolayer where there is little interaction between the adsorbed ions. The q_{max} value is also very similar to the experimental value of q_{max}. The Langmuir-Freundlich model fit the data the best of the competitive isotherm models having R^2 values of 0.89 and 0.83 for nickel and zinc respectively. This suggesting the binary adsorption has both Langmuir and Freundlich type behaviour.

Since the Langmuir model shows a better fit for the data and is simpler to model it would be the better model to use to analyse this system. As the binary system fit the Langmuir model best, the adsorption in the binary system most likely forms a monolayer with very little diffusion into the adsorbent.

4.6 Effect of pH on the adsorption of nickel and zinc

The alkalinity and the acidity of the solution have a great effect on the adsorption of metal ions onto the adsorbent. The adsorption of nickel, zinc, and binary solutions were carried out at 30 °C for 1 hour. The results are shown in Figure 14 where adsorption capacity, q_t, was plot against pH. Figure 15 shows the effect of pH on the individual components of the binary system.

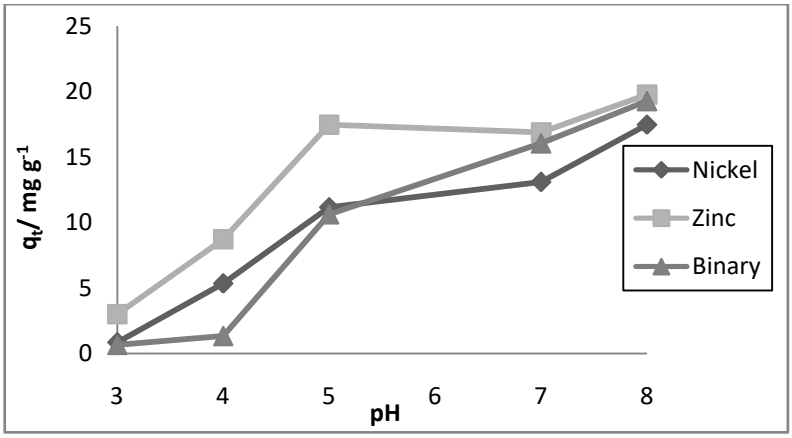

Figure 14. Adsorption capacity qt, of single system nickel, single system zinc and the binary system of nickel and zinc against various pH after 1 hour for an initial concentration of 50 mg/L at 30 °C

The adsorption capacity decreases greatly when the pH is decreased from the neutral pH 7 and when the pH was increased the adsorption increased. The plots of both nickel zinc adsorption shows the adsorption plateaus between pH 5-7. It was not possible to study the adsorption at a higher pH was at any pH value above 8 the zinc metal precipitated from the solution when they form insoluble metal hydroxide complexes.

This shows that at lower, more acidic environments adsorption decreases and the adsorption capacity was higher at higher pH, more basic environments. This was likely due to how the acid affects the functional groups on the adsorbent surface and therefore their effect on the adsorption mechanism.

At neutral pH the metal ion replaces a hydrogen atom on the surface functional group as shown in equation 22. At lower pH, more acidic environments there were higher concentrations of hydrogen ion, $[H^+]$. These ions, especially when in high concentrations protonate the surface functional groups, making the functional groups positively charged as shown in equation 23. This repelled the metal ions from the surface due to them having similar charges. The presence of hydrogen ions would also shift the equilibrium towards the side of the reactants.

When the pH was increased to pH 8 by the addition of sodium hydroxide, NaOH, the adsorption capacity increased. The hydroxide ions deprotonates the functional groups on the adsorbent surface making the functional groups positively charged which attracts the metal ions to the adsorbent surface shown as in equation 24.

$$\boldsymbol{ROH + M^+ \rightleftharpoons ROM + H^+} \qquad \textit{Eq. 22}$$

$$\boldsymbol{ROH + H^+ \rightleftharpoons ROH_2{}^+} \qquad \textit{Eq. 23}$$

$$\boldsymbol{ROH + OH^- \rightleftharpoons RO^- + H_2O} \qquad \textit{Eq. 24}$$

Nickel and zinc as well as the binary system were affected by the change in pH to similar extents. As shown in Figure 15 in the binary system the amount of adsorption for the nickel and zinc components were nearly identical, showing the change of pH and the effected it had on the adsorption mechanism affected both the mechanism

equally. From this we can deduce that the metals have similar adsorption mechanisms which are both affected by a change in pH.

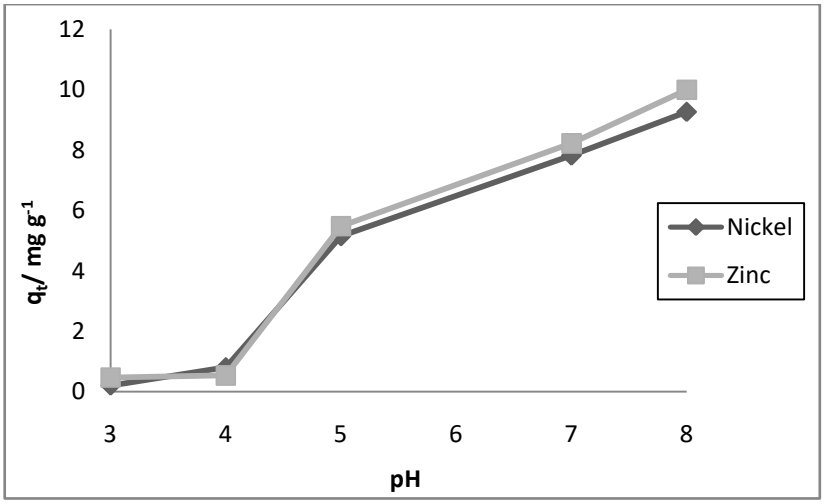

Figure 15. Adsorption capacity q_t of the nickel and zinc components against pH for the binary adsorption of concentration 50 mg/L after 1 hour at 30 °C

These experimental results are consistent with the literature. In a study by Ewecharoen et al. (2008) where the adsorption of nickel onto coir pith which showed the adsorption was lowest at pH 1-2 and highest amount of adsorption at pH 7. In a similar study by Amarasinghe (2011) where the adsorption of cadmium and lead onto coir pith was studied, the results suggests that adsorption increases with pH as there is very low adsorption at pH 1-2 and the most adsorption at pH 5-7. Very few of these studies show the effect of pH at pH values higher than 7, likely due to the possibility of precipitation of the metal ion complexes. Both nickel and zinc precipitate out of solution at around pH 9-10.

4.7 Kinetics of single system and binary system adsorption of nickel and zinc

4.7.1. Adsorption kinetics of single system nickel at various temperatures

A kinetic analysis was carried to study how nickel adsorption occurred as it approached equilibrium to determine the rate as well as determine the nature and mechanism of the adsorption. The adsorption of nickel onto coir pith over time at temperatures 30, 40, 50 and 60 °C was shown in Table 6. The equilibrium adsorption capacity q_{max} at 120 minutes as a function of temperature is shown in Figure 16. The adsorption of nickel at 30 °C increases until it reaches equilibrium adsorption capacity of 12.7 mg g^{-1}. The system at 40 °C shows initially more adsorption but it eventually decreases due to desorption occurring as it reaches equilibrium. At 60 °C nickel adsorption is initially very high but there is a lot of desorption as it approaches equilibrium.

Table 6. Adsorption capacities (q_t) of single system nickel at variable times at the temperatures of 30, 40, 50, and 60 °C (C_o= 50 mgL^{-1}, adsorbent dose= 0.75g)

q_t/mg g^{-1} time/ min	30 °C	40 °C	50 °C	60 °C
1	9.3	9.4	9.3	18.1
2	9.4	12.0	10.7	12.0
5	11.2	11.4	9.3	23.5
10	11.9	13.9	12.7	17.9
30	12.0	13.4	12.0	17.8
120	12.1	12.7	14.0	14.7

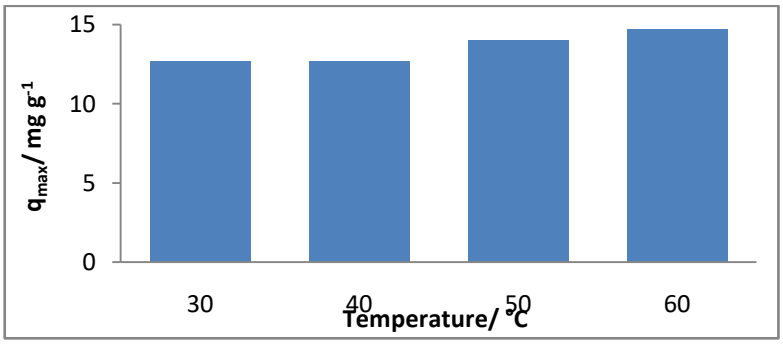

Figure 16. Equilibrium adsorption capacity, q_{max}, of single system nickel at 120 min as a function of temperature

The increase in equilibrium adsorption with the increase in temperature may be due to the adsorption process being endothermic or due to expansion of coir pith which gives a larger surface for adsorption resulting in more adsorption at higher temperatures. A similar trend was shown in a study by S. Ratan et al. (2016) who suggested that the increase in the adsorption of nickel onto chemically modified coir pith with increase in temperature was due to the increase in kinetic energy. This is consistent with what is seen in the nickel adsorption at 60 °C which had a much higher initial adsorption and slightly higher equilibrium adsorption capacity.

The data was analysed using the linear form of the Lagergren pseudo first order model (equation 9) by plotting the graph of $\ln(q_e-q_t)$ against time, t (min), as shown in Figure 17. The rate constant k_1 (min^{-1}) was estimated from the gradient and the equilibrium adsorption capacity was estimated from the intercept. The data fit poorly in the model resulting in low R^2 values. The data from the system at 60 °C could not be analysed as the experimental q_e value is lower than all the previous q_t values due to a significant amount of desorption occurring as the system reaches equilibrium resulting in (q_e-q_t) being negative. This was also the reason the system at 40 °C had only 3 data points in Figure 17.

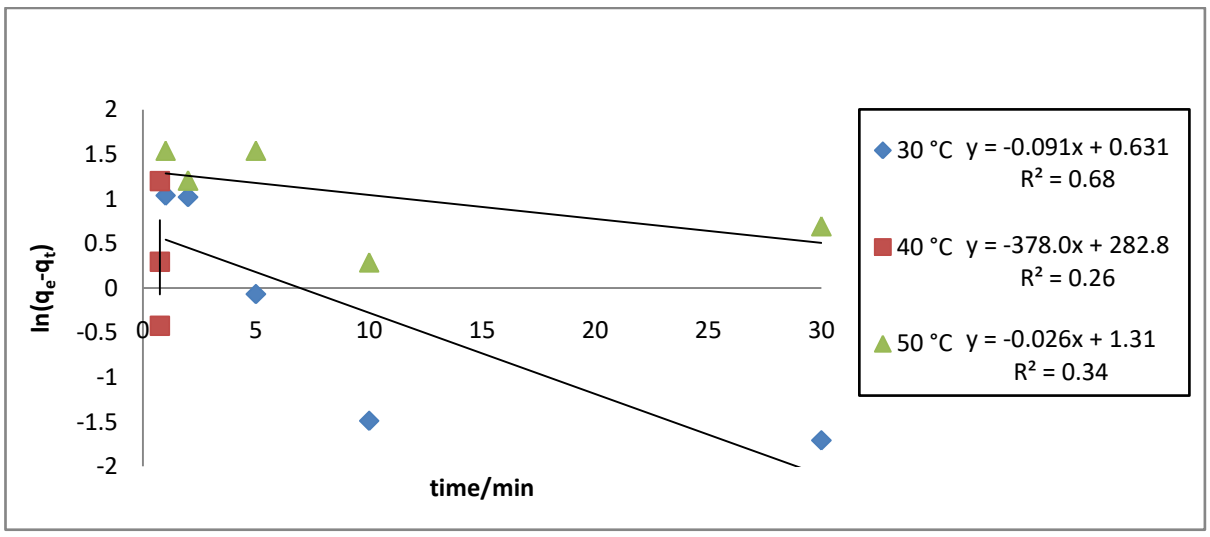

Figure 17. Plot of linearlized pseudo first order model analysis for the adsorption of nickel at temperatures of the $Ln(q_e-q_t)$ against time at 30, 40, 50 and 60 °C

The results were then analysed using the non-linear form of the Lagergren pseudo first order model and data fitting using the solver function in Excel. This analysis

also resulted in a poor fit so the results were not included. The poor fit of the data suggests that the model is unsuitable to analyse this system and that adsorption does not occur via physisorption.

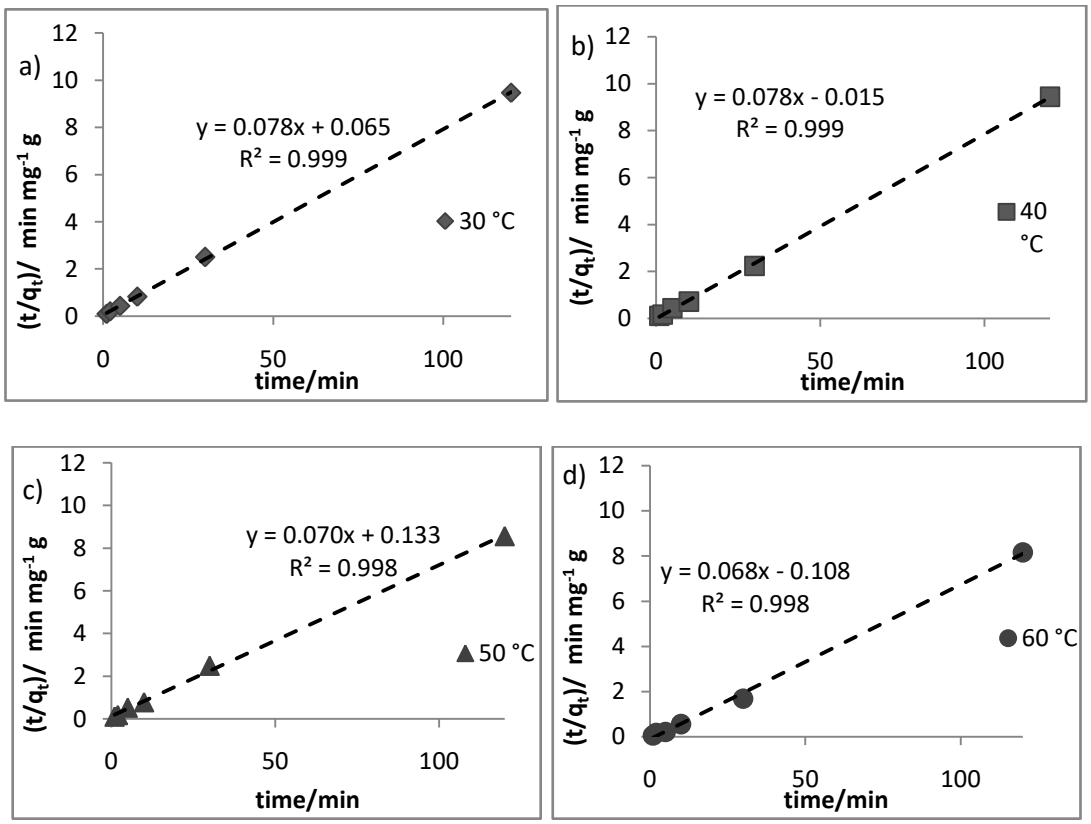

Figure 18.Plot of time divided by the adsorption capacity t/q_t for the linear form of the Lagergren pseudo second order analysis single system adsorption of nickel onto coir pith against time at a) 30 °, b) 40 °C, c) 50 °C, d) 60 °C

The data was then analysed using the linear form of the Lagergren pseudo second order model (equation 11) by plotting t/q_t (min $mg^{-1}g$) against time, t (min) as shown in Figure 18 where equilibrium adsorption capacity was estimated from the gradient and the rate constant, k_2 (g mg^{-1} min^{-1}) was estimated from the intercept. The R^2 for the data was 0.99 at all the temperatures, the calculated values of q_e match very closely to the experimental values shown in Table 7. The decrease in k_2 value with the increase in temperature suggests either the rate of adsorption decreases or that the rate of desorption increases with temperature.

Table 7.Kinetic constants of nickel adsorption determined by the Lagergren pseudo second order analysis

Temperature/^{o}C	h_{exp}/ mgg^{-1} min^{-1}	$q_{e\ (exp)}$/mgg^{-1}	$q_{e(pred)}$/mgg^{-1}	k_2/ mg^{-1}gmin^{-1}	R^2
30	25	12.67	12.20	0.20	0.99
40	21	12.70	12.82	-0.41	0.99
50	17	14.00	14.29	0.04	0.99
60	83	14.70	14.71	-0.04	0.99

For the system at 40 ^{o}C and 60 °C, possibly due to the desorption that occurs the k_2 value was negative due to the desorption which occurs as the system reaches equilibrium. The values of k_2 and q_e were used to calculate lines of regression as shown in Figure 19.

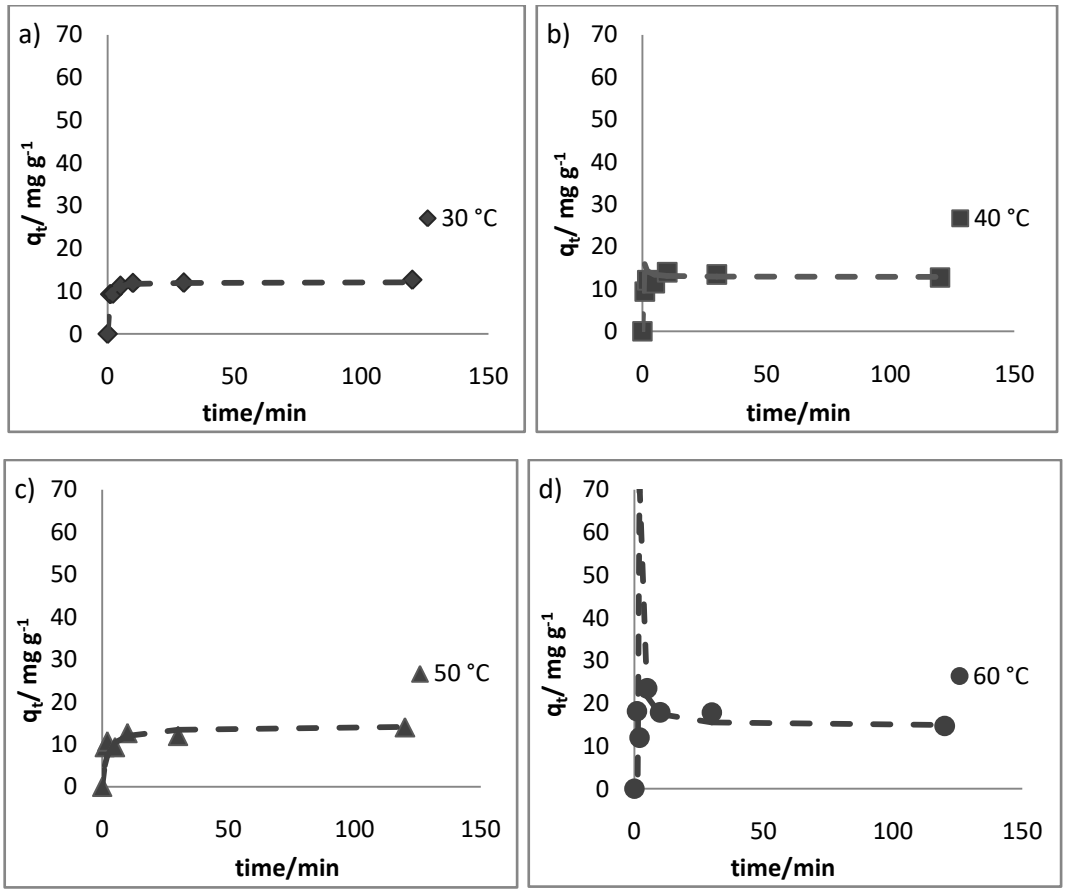

Figure 19.Plot of the adsorption capacity q_t for the single system adsorption of nickel onto coir pith against time at a) 30 ^{o}, b) 40 ^{o}C, c) 50 ^{o}C, d) 60 ^{o}C for nickel with an initial concentration of 50 mg L^{-1}.

The best method to analyse the adsorption data would be to use the linear form of the Lagergrem Pseudo second order model. As the data was very consistent with this model the adsorption occurs via chemisorption.

The kinetic data of nickel adsorption at various temperatures was then analysed using the intraparticle diffusion model (equation 13). The data for the adsorption of nickel at 30 °C was shown in Figure 20 where adsorption capacity at a given time, q_t (mgg^{-1}), was plot against the square root of time, $t^{1/2}(min^{1/2})$. The plot was multi-linear with two distinct lines intersecting with the line not intersecting the origin. From this we can deduce the adsorption process is influenced by two or more steps. Majority of the adsorption occurs via external mass transfer with intra-particle diffusion being slower. After intraparticle diffusion step there is very little adsorption, likely due to saturation of the adsorbent suggesting only macroporous diffusion occurs. The intercept of the first line 7.858 mg g^{-1} is proportional to the boundary layer thickness, is larger due to the external mass transfer effect. The gradient of the first line is the rate parameter of the intraparticle diffusion which is 1.328 mg g^{-1} $min^{-1/2}$.

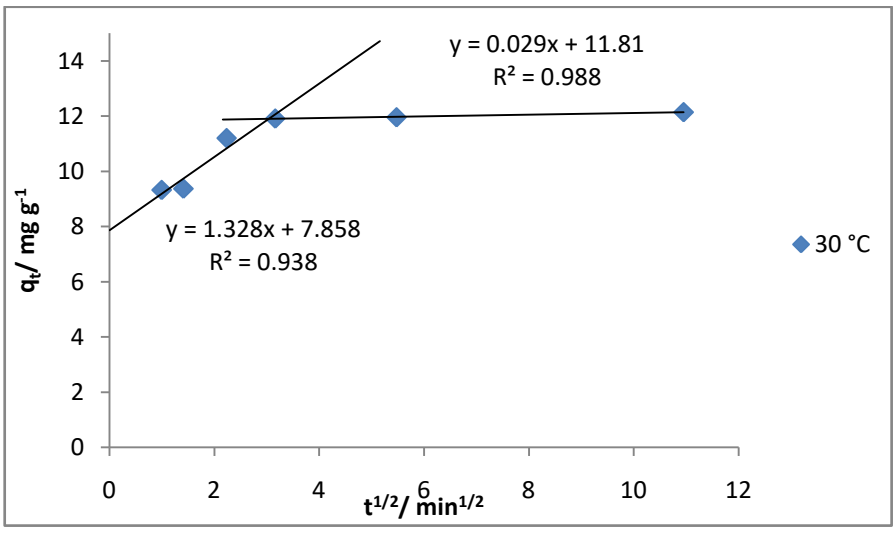

Figure 20.Intraparticle diffusion model of nickel at 30 °C

Figure 21 shows the analysis of the nickel adsorption data at 40 °C by the intraparticle diffusion model with adsorption capacity against the square root of time. Similarly to the adsorption at 30 °C adsorption occurs in distinct steps, first a quick external mass transfer step. However unlike the previous system after the intraparticle diffusion desorption occurs as the system reaches equilibrium. The boundary layer thickness is proportional to 8.382 mg g^{-1} and the rate parameter is 1.688 mg g^{-1} $min^{-1/2}$.

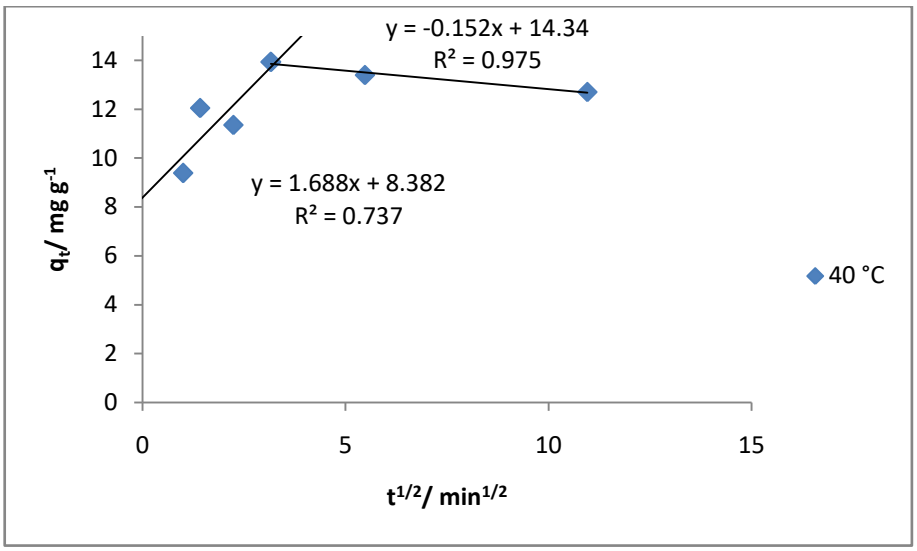

Figure 21.Intraparticle diffusion model of nickel 40 °C

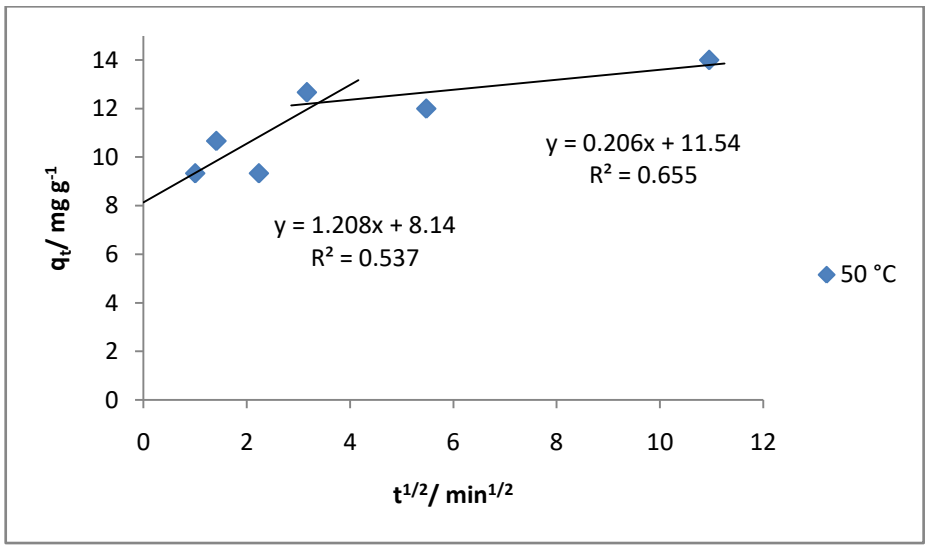

Figure 22.Intraparticle diffusion model of nickel adsorption at 50 °C

When the temperature was increased further there are more distinct steps as shown in Figure 22. Unlike the previous systems after the fast external mass transfer, the slower intraparticle diffusion step is followed by a significant amount of intraparticle diffusion as it reaches equilibrium. This means there is both macroporous and microporous diffusion and is likely due to the expansion of the pores of the adsorbent as the temperature increases resulting in more diffusion.

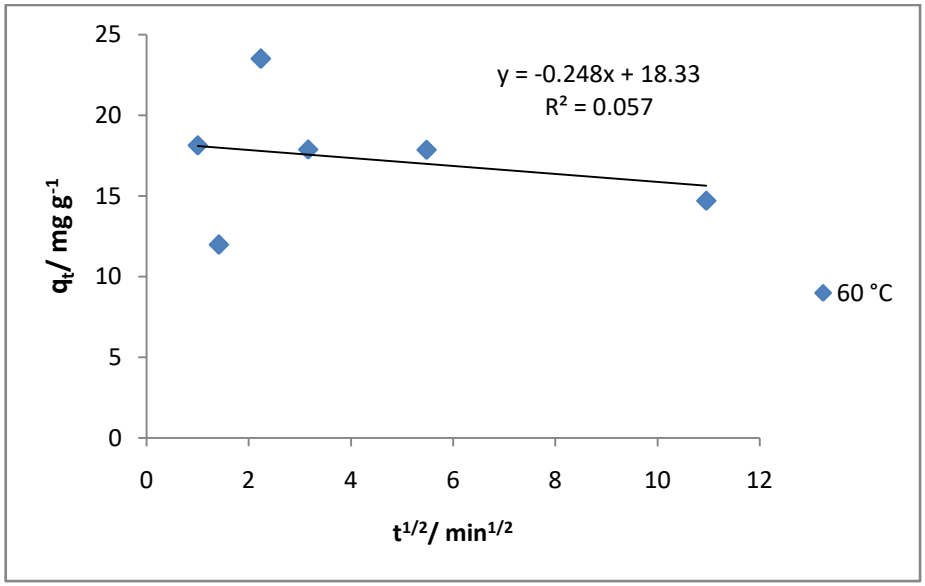

Figure 23.Intraparticle diffusion model of nickel adsorption at 60 °C

For the adsorption of nickel at 60 °C as shown in Figure 23 there is little to no intra-particle diffusion. In fact it was primarily desorption occurring after the initial mass transfer. The data for this system fit poorly into the intraparticle diffusion model due to the erratic way adsorption and desorption occurred. It is likely that while the higher temperature causes the adsorbent to expand which increases adsorption it also cases a increase in kinetic energy which favour more desorption, the overall result is which of these two is more significant.

As shown in Table 8 the rate of intraparticle diffusion (k_{id}) decreases with temperature while the constant (c) which is proportional to the boundry layer thickness c increases with temperature so while the adsorption of nickel is favoured by higher temperatures the intraparticle diffusion decreased. This means as

temperature increases chemisorption onto the surface is preferred to diffusion into the adsorbent pores.

Table 8.Constants determined using the intraparticle diffusion model

Temperature/ ^{o}C	k_{id}/ mg g^{-1} $min^{-1/2}$	c/ mg g^{-1}	R^2
30	1.33	7.86	0.94
40	1.69	8.38	0.74
50	1.21	8.14	0.54
60	-0.25	18.33	0.06

4.7.2 Adsorption kinetics of single system zinc at various temperatures

A kinetic analysis was carried to study how zinc adsorption occurred as it approached equilibrium to determine the rate as well as determine the nature and mechanism of the adsorption.

Table 9. Adsorption capacities (q_t) of single system zinc at variable times at the temperatures of 30, 40, 50, and 60 °C (C_o= 50 mgL^{-1}, adsorbent dose= 0.75g)

q_t/mg g^{-1} / time/ min	30 °C	40 °C	50 °C	60 °C
1	8.7	13.4	14.7	12.0
2	9.4	14.7	10.0	11.3
5	9.9	13.3	9.3	10.7
10	16.8	16.6	11.3	7.3
30	18.7	16.6	10.7	13.3
120	17.9	16.6	7.7	7.4

The adsorption of zinc at 30 °C increases until it reaches equilibrium. The system at 40 °C has less adsorption but the systems reaches equilibrium faster as shown in Table 9. As temperature increases there is a decrease in equilibrium adsorption capacity as shown in Figure 24.

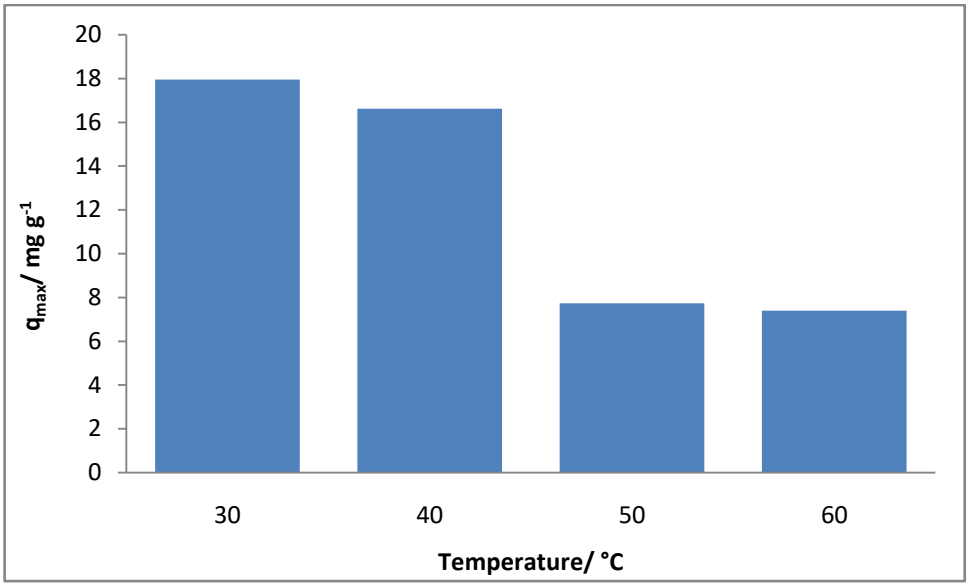

Figure 24. Equilibrium adsorption capacities, q_{max}, of zinc at 120 min as a function of temperature

The decrease in adsorption with temperature is likely due to the increased kinetic energy of the metal ions at higher temperatures resulting in more desorption. There is more initial adsorption when the temperature is increased due to an increase in kinetic energy for the metal ions but there is also an increases the rate of desorption as time goes on. Higher temperatures may result in an expansion of the pores of the adsorbent which would result in more adsorption yet the dominate effect is the increased kinetic energy which leads to some desorption.

The data was analysed using the linear form of the Lagergren pseudo first order model (equation 9) by plotting the graph of $\ln(q_e-q_t)$ against t as shown in Figure 25. When the temperature was increased from 30 ^oC to 40 ^oC the rate constant k_1 increased from 0.229 to 0.557 min^{-1} likely due to the increase in kinetic energy of the system. The values of q_e calculated from the plot did not match the experimental values of q_e of the adsorption at 30 ^oC and 40 ^oC.

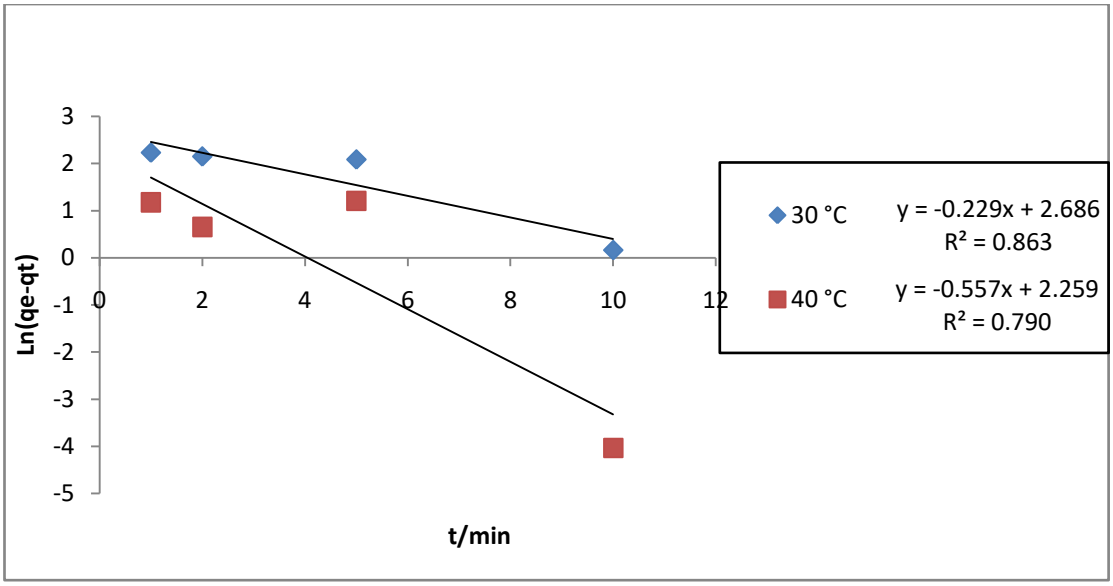

Figure 25.Plot of linearlized pseudo first order model analysis for the adsorption of zinc at temperatures of the Ln(q_e-q_t) against time at 30, 40, 50 and 60 °C

The data for the adsorption at 50 and 60 °C could not be analysed using this method due to desorption that occurs in these systems the equilibrium adsorption capacity (q_e) values is less than the preceding adsorption capacity (q_t) values. The data was then analysed using the non-linear form of the Lagergren pseudo first order model and the solver function in Excel. This analysis also resulted in a poor fit so the results were not included. The poor fit of the data suggests that the model is unsuitable to analyse this system and that adsorption does not occur via physisorption.

The linear form of the pseudo second order model was used to analyse the kinetic data by plotting t/qt against time a4s shown in Figure 26. The correlation coefficient for all the different temperature systems were 0.99 showing a very good fit of the data to the model as shown in Table 10. The calculated values of q_e also matched closely to the experimentally obtained values of q_e. The rate constant k_2 showed that rate increased when the temperature was increased from 30 to 40 °C due to increase in kinetics of the metal ions but then decreased to negative values when the temperature was increased further due to desorption and the destabilisation of the bond between the metal ion and the adsorbent.

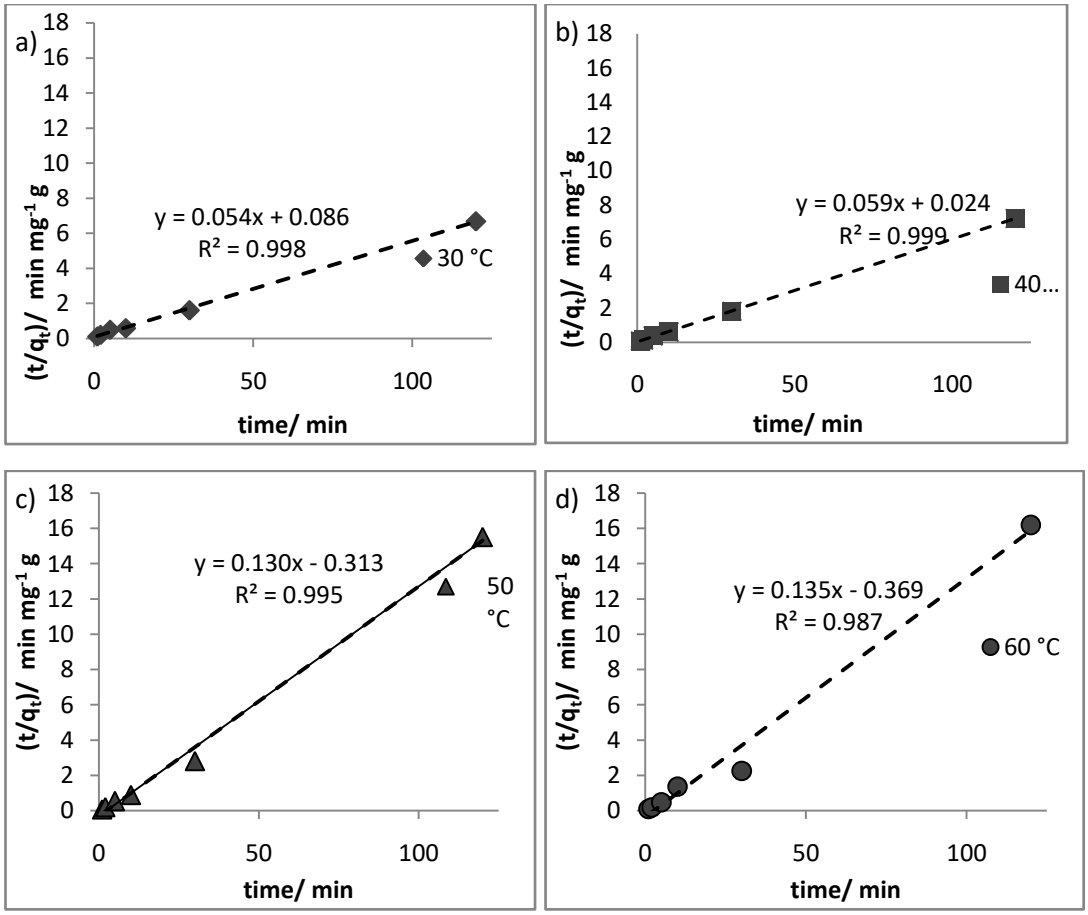

Figure 26. Plot of time divided by the adsorption capacity t/qt for the linear form of the Lagergren pseudo second order analysis single system adsorption of zinc onto coir pith against time at a) 30 °, b) 40 °C, c) 50 °C, d) 60 °C

Table 10. Kinetic constants of single system zinc adsorption determined by the Lagergren pseudo second order analysis

Temperature/°C	h_{exp}/mgg^{-1}min^{-1}	$q_{e\ (exp)}$/mgg^{-1}	$q_{e\ (pred)}$/mgg^{-1}	k_2/ mg^{-1} g min^{-1}	R^2
30	14.08	17.95	18.52	0.034	0.99
40	55.56	16.63	16.94	0.145	0.99
50	90.90	7.73	7.35	-0.05	0.99
60	-13.88	7.41	7.407	-0.049	0.99

The best method to analyse the adsorption data would be to use the linear form of the Lagergrem Pseudo second order model. As shown in Figure 27 where the regression line plot using the values deduced from the model against the experimental data thus it can be inferred that the adsorption occurs via chemisorption.

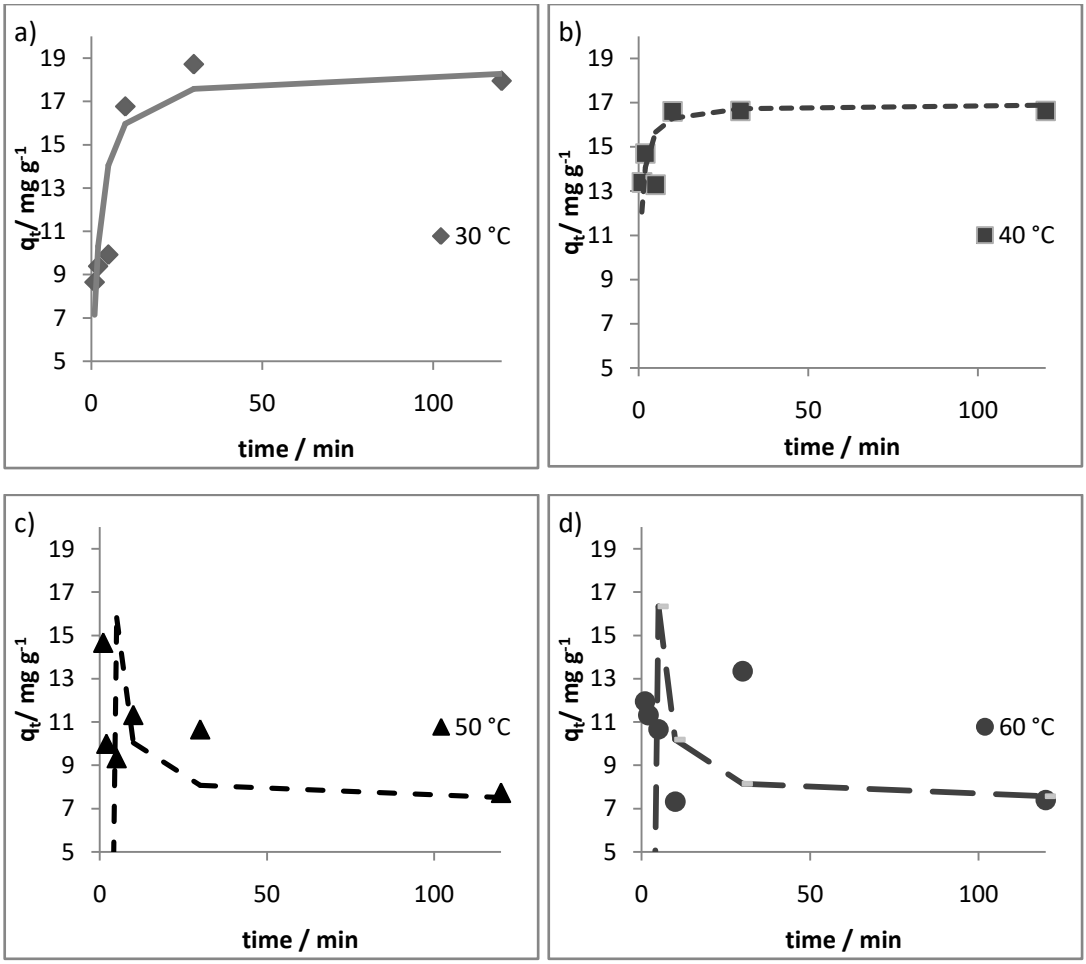

Figure 27. Plot of the adsorption capacity q_t for the single system adsorption of zinc onto coir pith against time at a) 30 °, b) 40 °C, c) 50 °C, d) 60 °C for zinc with an initial concentration of 50 mg L^{-1}

The kinetic data of zinc adsorption at various temperatures was then analysed using the intra particle diffusion model.

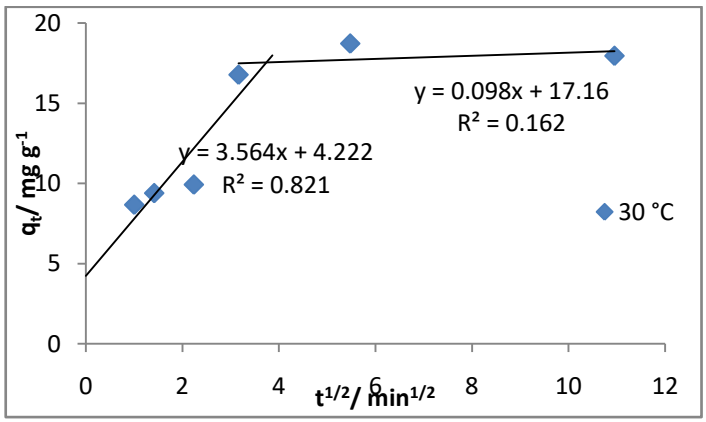

Figure 28.Intraparticle diffusion model of zinc adsorption at 30 °C

The data for the adsorption of nickel at 30 °C was shown in Figure 28 where adsorption capacity at a given time, q_t (mg g^{-1}) was plot against the square root of time, $t^{1/2}$ ($min^{1/2}$). The plot was multi-linear with two distinct lines intersecting with the line not intersecting the origin. From this we can deduce the adsorption process is influenced by two or more steps. Majority of the adsorption occurs via intraparticle diffusion as this system has boundary layer thickness of 4.22 mg g^{-1}. After intraparticle diffusion step there is very little adsorption, likely due to saturation of the adsorbent suggesting only macroporous diffusion occurs. The gradient of the first line is the rate parameter of the intraparticle diffusion which is 3.364 mg g^{-1} $min^{-1/2}$.

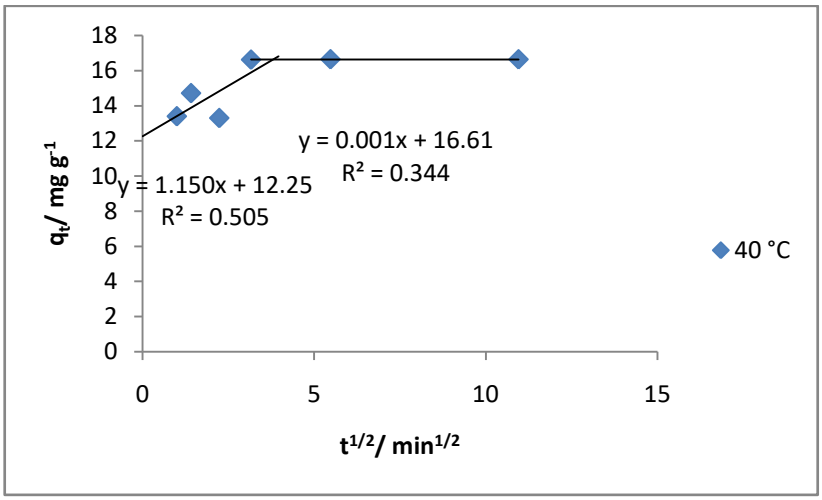

Figure 29.Intraparticle diffusion model of zinc adsorption at 40 °C

When compared to the system at 30 °C the system at 40 °C as shown in Figure 29 still has two distinct adsorption steps yet the majority of adsorption has occurred in the external mass transfer step with the boundary layer thickness being larger at 12.25 mg g^{-1}. The amount of intraparticle diffusion and rate of it decreased at the higher temperature.

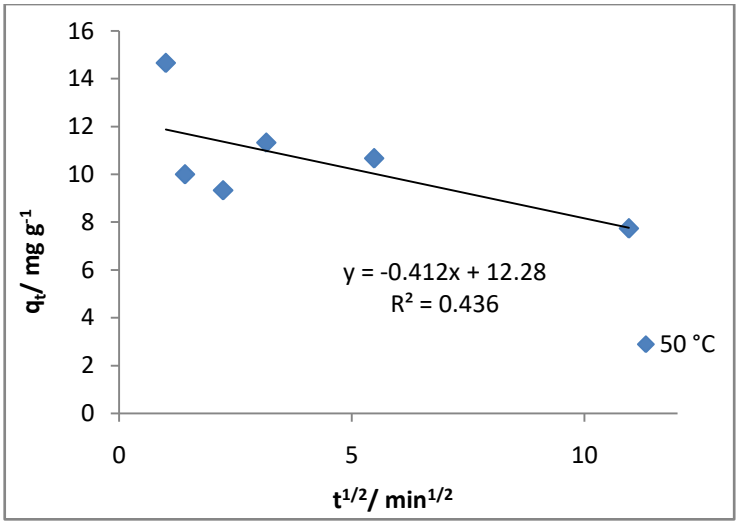

Figure 30.Intraparticle diffusion model of zinc adsorption at 50 °C

In the system at 50 °C and 60 °C as shown in Figure 30 and Figure 31 there is no observable intraparticle diffusion due to primarily desorption taking place after the initial external mass transfer step. The regression lines have a poor fit which means this system likely does not undergo any intraparticle diffusion. Constants determined using the intra particle diffusion modelare shown in Table 11.

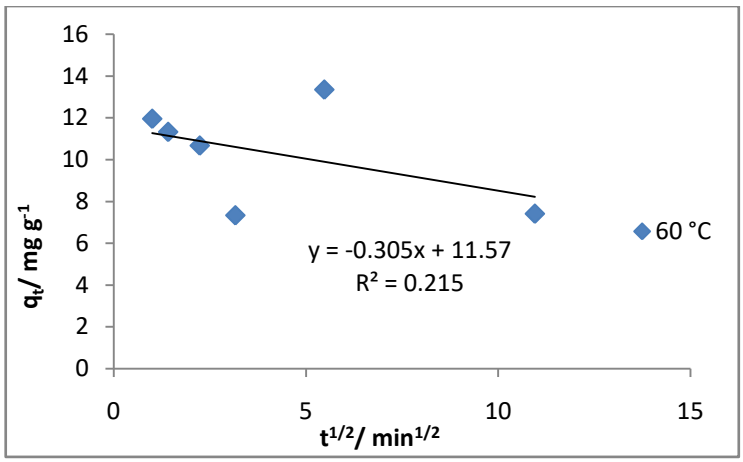

Figure 31.Intraparticle diffusion model of zinc adsorption at 60 °C

Table 11. Constants determined using the intra particle diffusion model

Temperature/ °C	**k_{id}/ mg g^{-1} $min^{-1/2}$**	**c/ mg g^{-1}**	**R^2**
30	3.56	4.22	0.82
40	1.150	12.25	0.51
50	-0.412	12.28	0.44
60	-0.305	11.57	0.22

4.7.3 Kinetic analysis of the binary system at various temperatures

The total adsorption is the summation of the nickel and zinc adsorption and the overall effect of being in a binary system. A kinetic analysis was carried to study how the binary adsorption occurred as it approached equilibrium to determine the rate as well as determine the nature and mechanism of the adsorption.

The adsorption at 30 °C had a slow rate but was primarily adsorption until it reached equilibrium. When the temperature was increased the initial adsorption was greater but desorption occurred as the system reached equilibrium as shown in Table 12.

Table 12. Binary adsorption capacities q_t of variable times at the temperatures of 30, 40, 50, and 60 °C

q_t/mgg^{-1}	30 °C			40 °C			50 °C			60 °C		
time/min	Ni	Zn	Total	Ni	Zn	Total	Ni	Zn	Total	Ni	Zn	Total
1	7.9	6.6	14.5	4.0	4.0	8.0	9.4	10.0	19.4	11.1	11.0	22.1
2	5.3	6.0	11.3	6.0	6.0	12.0	8.0	8.7	16.6	9.3	10.0	19.3
5	6.0	5.3	11.3	4.7	4.7	9.4	8.0	7.3	15.3	9.3	9.3	18.6
10	6.6	5.3	12.0	5.3	5.3	10.6	10.8	10.1	20.9	8.6	9.3	17.9
30	6.0	4.6	10.6	6.7	8.0	14.7	8.7	8.0	16.7	10.0	10.5	20.6
120	6.7	7.3	14.0	7.3	4.0	11.3	6.0	4.0	10.0	6.0	2.7	8.7

Overall the rate and amount of initial adsorption due to external mass transfer increased with temperature but the equilibrium adsorption decreased as shown in Figure 32. This was possibly due to the increase in temperature increasing the rate as well as causing the pores in the adsorbent to increase but also weakening the attraction between the metal ion and the adsorbent due to increase in the kinetic energy. It is likely that the binary adsorption is exothermic.

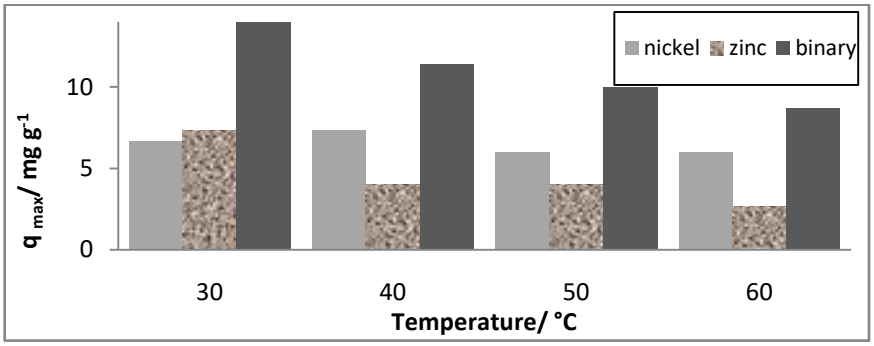

Figure 32. Equilibrium adsorption capacities of the total binary system and their nickel and zinc components at each temperature

The data was first analysed using the linear Legergren pseudo first order model as shown in Figure 33. The data for the binary adsorption at 30 °C fit the model poorly and likely had little to no physisorption occurring. The system at 40 °C showed a better fit but that was likely due to only three data points being usable as due to desorption occurring as the system reached equilibrium several of the preceding q_t values could not be analysed using this model. The data for the adsorption could not be analysed for systems at 50 and 60 °C as all the q_t values were larger than the q_e values.

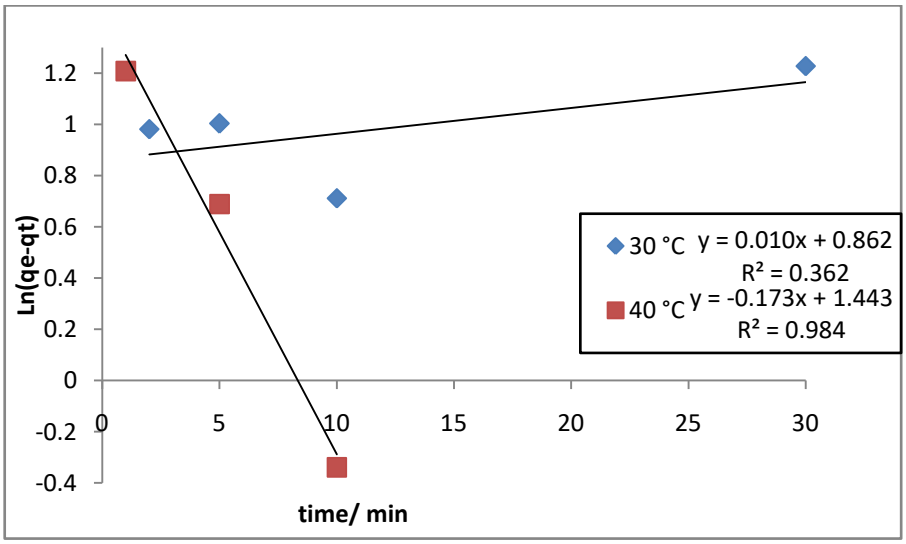

Figure 33. Plot of the linear Lagergren Pseudo first order model analysis of the adsorption data for the binary adsorption of nickel and zinc at 30, 40, 50 and 60 °C

The data was then analysed using the linear form of the Lagergren Pseudo second order model which is used to model for chemisorptions where the metal ion forms a chemical bond with the functional groups on the adsorbent surface. The models fit well for the adsorption at all the temperatures as shown in Figure 34 where the correlation coefficients were all close to 1.

The calculated values of the equilibrium adsorption capacity matched closely with the experimental values as shown in Table 13. The rate constant decreases when the temperature was increased from 30 °C, the negative value of the k_2 values for the systems at higher temperatures is due to the desorption that occurs at it reaches equilibrium.

Table 13.Kinetic constants of binary adsorption determined by the Lagergren pseudo second order analysis

Temperature /°C	h_{exp}/ mg g^{-1} min^{-1}	$q_{e\ (exp)}$/ mg g^{-1}	$q_{e(pred)}$/ mg g^{-1}	k_2/ mg^{-1} g min^{-1}	R^2
30	5.88	14.00	14.08	0.03	0.99
40	83.33	11.34	11.49	-0.14	0.99
50	52.63	9.99	9.90	-0.03	0.99
60	-142.85	8.67	8.55	-0.02	0.98

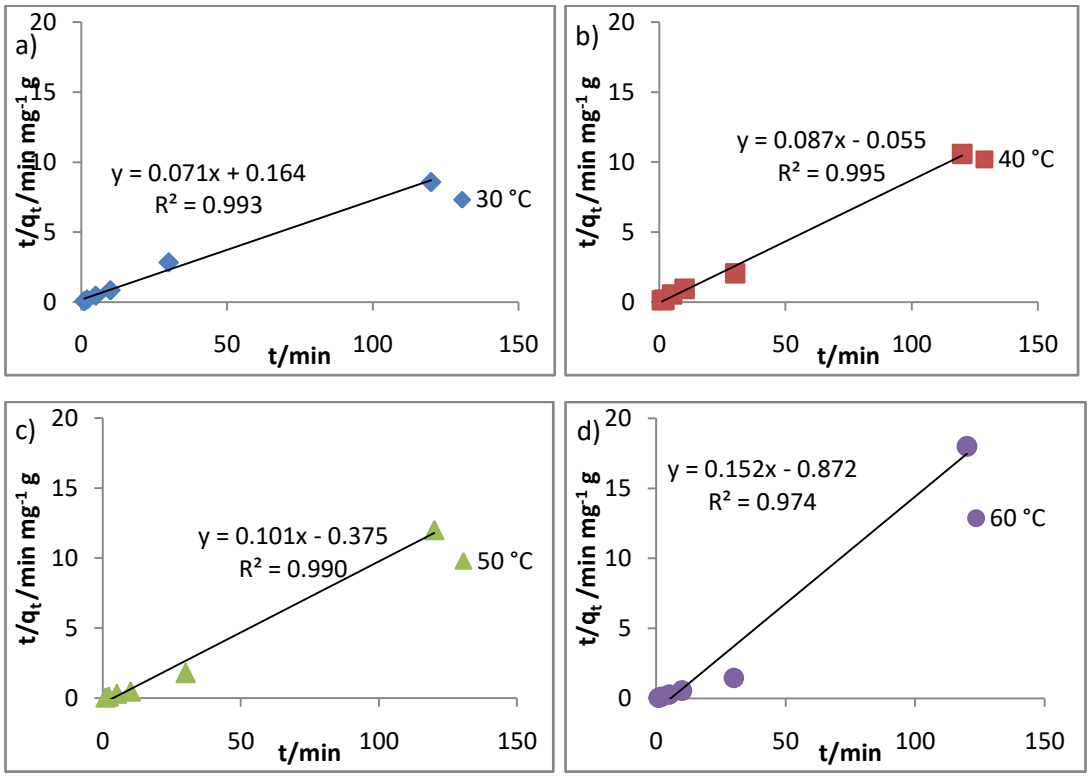

Figure 34.Plot of the linear Lagergren Pseudo second order model analysis of the adsorption data for the binary adsorption of nickel and zinc at a) 30°C, b) 40°C, c) 50°C and d) 60 °C

Using the values calculated using the Lagergren pseudo second order model regression lines were plot against the experimental data as shown in Figure 35. As the lines have a reasonable fit and shapes consistent with the data points it can be deduced that adsorption occurs by chemisorptions.

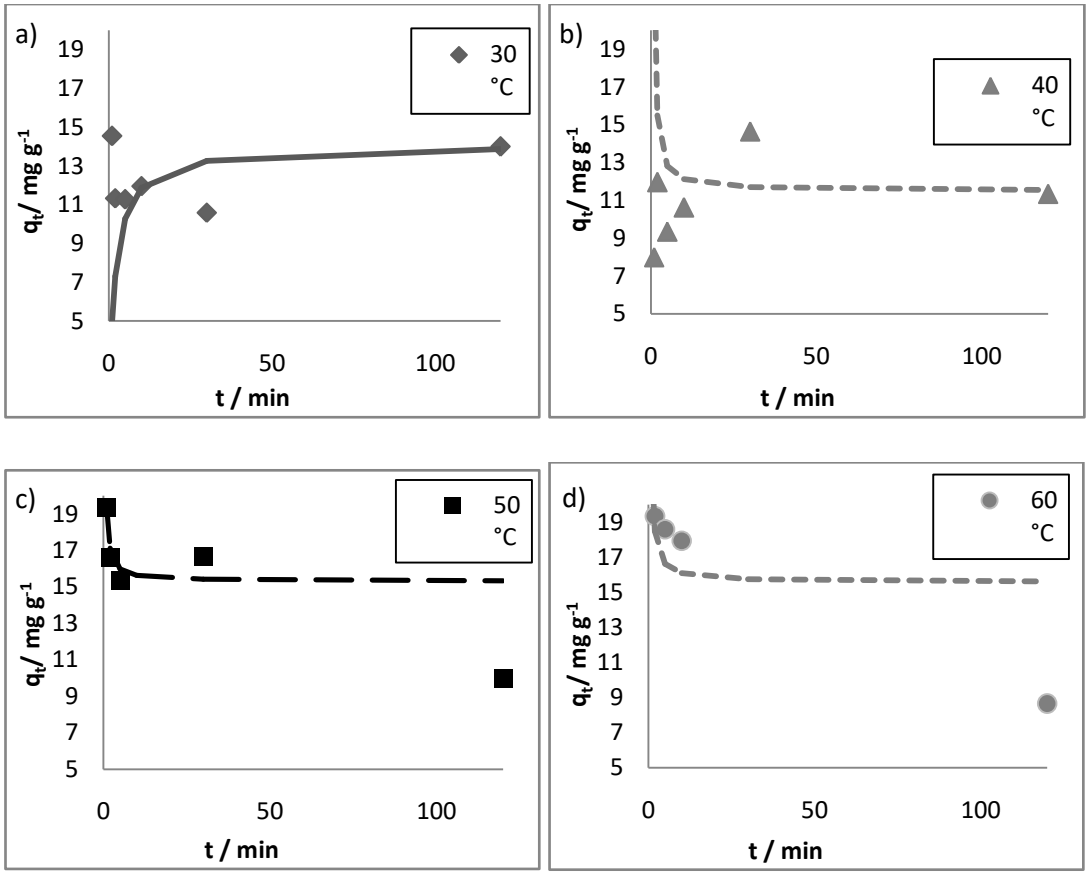

Figure 35.Adsorption capacity against time for the adsorption in the binary system at a)30°C, b)40°C, c)50 °C and d)60 °C with an initial concentration of 50 mg L^{-1} with a nickel to zinc ratio of 1:1

The binary adsorption data was analysed using the Intraparticle diffusion model as shown in Figure 36 for the binary adsorption at 30, 40, 50 and 60 °C. The binary adsorption system at 30 °C show little to no intraparticle diffusion with the regression line fitting the data poorly. The system at 40 °C shows some intraparticle diffusion, likely due to the expansion of pores of the adsorbent due at the increased temperature promoting intraparticle diffusion. However as the system reaches equilibrium there is desorption, possibly reversing the intraparticle diffusion. At 50 and 60 °C there is no intraparticle diffusion, instead desorption occurring after the initial external mass transfer step.

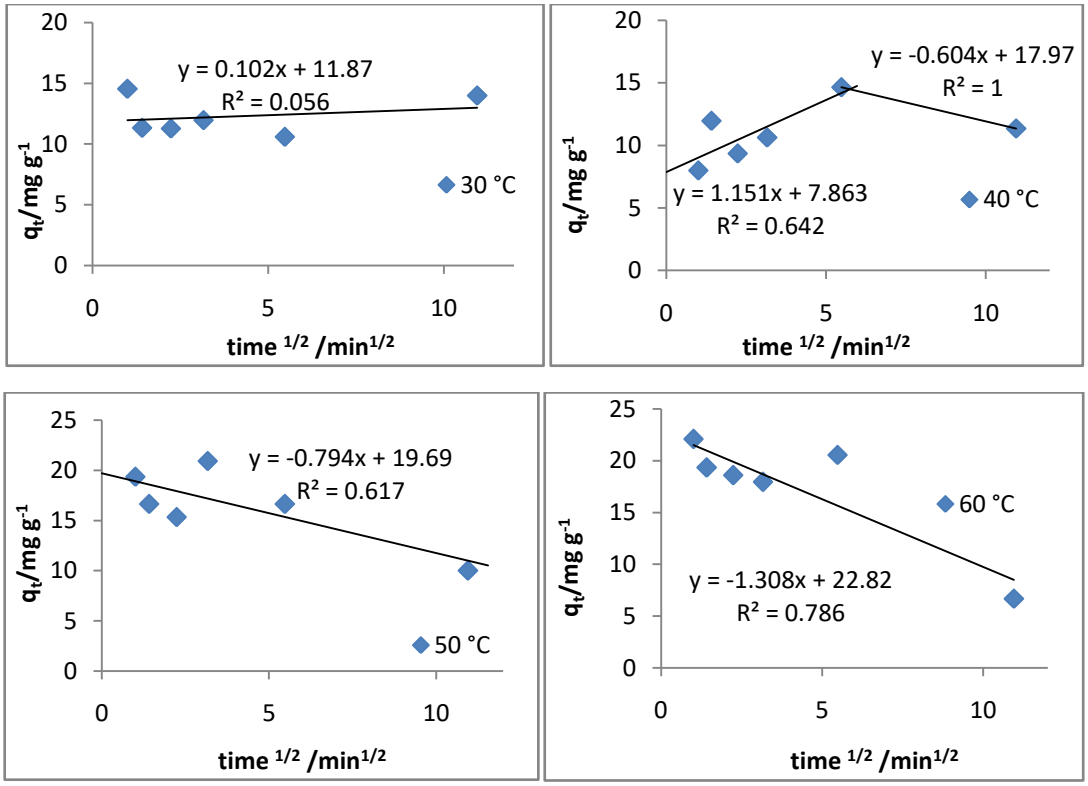

Figure 36.Intraparticle diffusion model of binary adsorption at a)30 °C, b)40 °C, c)50 °C, d)60°C

As the data fits the intraparticle diffusion model poorly it can be deduced that little to no intraparticle diffusion occurs. This would seem consistent with the mechanism deduced from the isotherm analysis which suggests in the binary system metal ions adsorb onto the adsorbent surface as a monolayer and there is no adsorption after the monolayer forms.

4.7.4 Analysis of the nickel and zinc components of the binary adsorption

To study how the nickel and zinc components of the binary system behave the equilibrium adsorption capacity was plot against the temperature for the nickel and zinc components as shown in Figure 37.

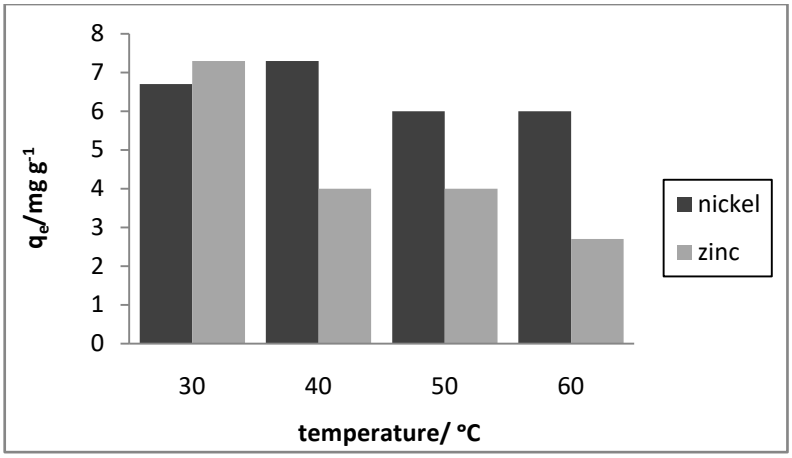

Figure 37.Equilibrium adsorption capacity against temperature of the nickel and zinc components of the binary adsorption

The equilibrium adsorption capacity was highest at 30 °C and decreased at higher temperatures. The adsorption of nickel does not change drastically, increasing slightly at 40 °C and decreasing slightly as the temperature increased further. Zinc adsorption however decreased greatly as temperature increased. At 30 °C there was more zinc adsorption than nickel adsorption but as temperature increased there was more nickel adsorption than zinc adsorption. It is likely that the presence of other metal ions decrease adsorption, this effect is exacerbated when the temperature increases and effects zinc adsorption more than it affects nickel adsorption.

This antagonism suggests nickel and zinc share the same adsorption sites and the bond formed between nickel and the adsorbent is stronger than that formed between zinc and the adsorbent. The individual components of the binary system were analysed using the Lagergren pseudo second order model and the intra-diffusion model. The Lagergren pseudo first order model was not used as the model fit poorly for both the binary and the single system data.

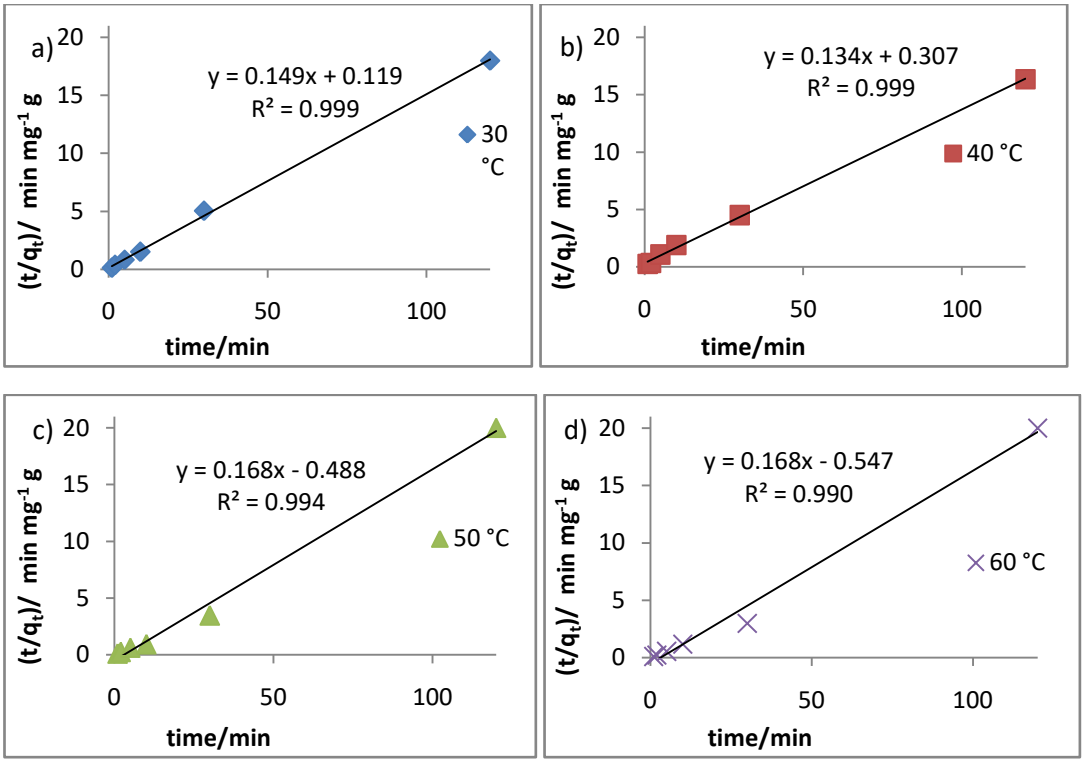

Figure 38. Plot of the linear Lagergren Pseudo second order model analysis of the adsorption data for the nickel component of the binary adsorption at a) 30, b) 40, c) 50, and d) 60 °C

Figure 38 and 39 shows the Lagergren pseudo second order analysis of the nickel and zinc components of the binary adsorption at various temperatures respectively. The linear form of the model was used and showed to have a good fit and a high correlation coefficient for all the data. The parameters of rate $k_2$and equilibrium adsorption capacity, q_e calculated using these plots are shown in Table 14.

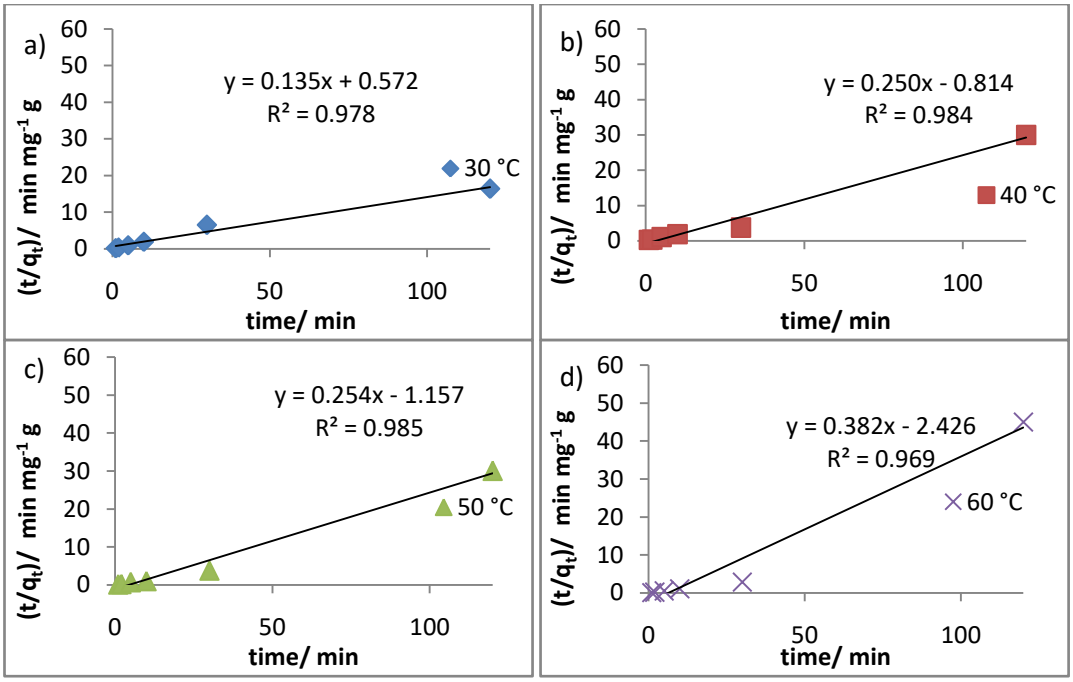

Figure 39. Plot of the linear Lagergren Pseudo second order model analysis of the adsorption data for the zinc component of the binary adsorption at a) 30, b) 40, c) 50, and d) 60 °C

Table 14. Analysis of the nickel and zinc components of the binary adsorption by Lagergren Pseudo second order model at 30, 40, 50, and 60 °C

	Temperature/°C	$q_{e\,(exp)}$/mg g^{-1}	$q_{e(pred)}$/mg g^{-1}	k_2/ mg^{-1} g min^{-1}	R^2
Nickel	30	6.67	6.70	0.186	0.99
	40	7.34	7.46	0.058	0.99
	50	5.99	5.95.	-0.057	0.99
	60	6.00	5.95	-0.516	0.99
Zinc	30	7.33	7.41	0.031	0.98
	40	4.00	4.00	-0.076	0.98
	50	3.99	3.93	-0.056	0.99
	60	2.67	2.61	-0.06	0.97

When the data for the nickel and zinc components of the binary adsorption system was analysed using the intraparticle diffusion model it was shown to have poor fit and relatively low correlation coefficient. For both the nickel and zinc components the rate of diffusion, k_{id}increases when the temperature increases to 40 °C and decreases when the temperature is increased further. Overall the boundary layer thickness, C, increases as the temperature increases. This all shows there is little to

no intraparticle diffusion in this adsorption system, even less when the temperature increases and more diffusion occurs.

4.7.5 Comparing the adsorption of single system nickel and single system zinc with the binary system at various temperature

During adsorption there are several steps and mechanism which occur that effect the extent of adsorption taking place as the system reaches equilibrium. The nickel adsorption, zinc adsorption and the binary adsorption all differ from each other but are similar as they share similar mechanisms of adsorption. The concentration of the solution, the mass of the adsorbent, the temperature of the solution and the contact time effect the external mass transfer, the intraparticle diffusion and the adsorption-desorption equilibrium.

The differences in the size and charge density of the nickel and zinc ions result in there being more zinc adsorption than nickel adsorption under similar conditions. Nickel is smaller and more highly charged therefore would prefer the more polar environment of the water as opposed to the adsorbent surface. In the binary system, in addition to afore mentioned conditions the interactions between the nickel and zinc metal ions affect the adsorption as well.

In Figure 40 equilibrium adsorption of the nickel, zinc and the binary system at different temperatures is shown. At 30 °C the equilibrium adsorption of the binary system is approximately equal to the average of the nickel and zinc values of equilibrium adsorption capacity. This suggests at 30 °C the presence of other metal ions does not greatly impact the amount of adsorption. However that from this graph the type and strength of the bonds formed during adsorption cannot be evaluated only the amount of adsorption occurring.

For the nickel and zinc single systems when the temperature increased, the equilibrium adsorption capacity increased slightly until 50 °C and then decreased when the temperature was increased further to 60 °C. Yet for the binary system at the adsorption decreases when the temperature increases suggesting that as the temperature increases the strength of the bonding is much weaker and desorption

occurs more easily. It is only likely that the presence of competitive species promote desorption more at higher temperatures as the total binary adsorption is much less than the average of the nickel and zinc systems.

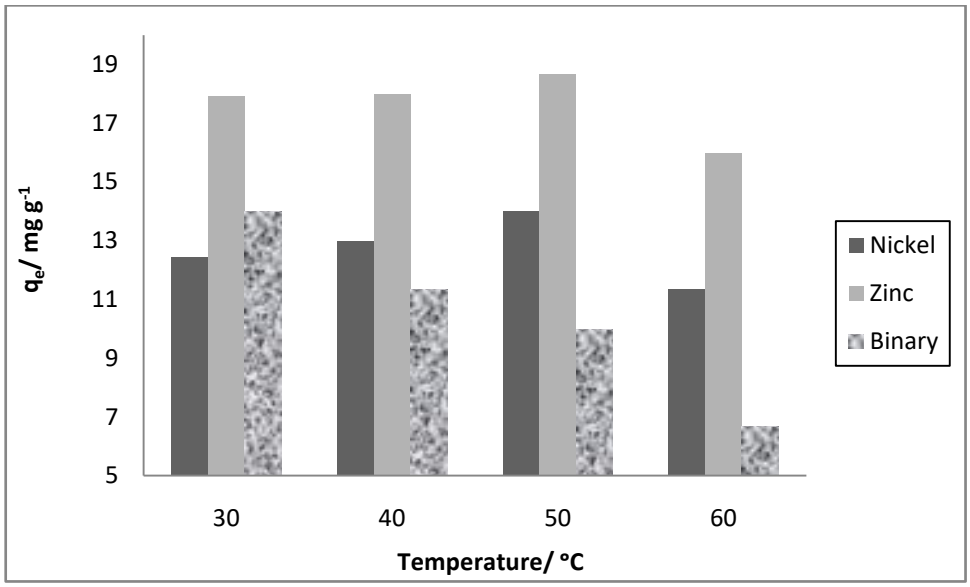

Figure 40.Equilibrium adsorption capacity against temperature of the adsorption of nickel, zinc and the binary system with an initial concentration of 50 mg L^{-1}

In the single system, the adsorption of zinc at the lower temperatures is much higher than nickel at lower temperatures while in the binary system they have roughly equal adsorption at 30 °C as shown in Figure 37 and Figure 40. Similar to the single system the adsorption of zinc decreases with temperature in the binary system as well as shown in Figure 37. The adsorption of nickel increases with temperature in the single system but decreases in the binary system, the adsorption of nickel is preferred to the adsorption of zinc at higher temperatures.

This was further illustrated in Figure 41 where q_e (mg g^{-1}) is the equilibrium adsorption capacity of the metal ion component in the binary system and q_m (mg g^{-1}) is the equilibrium adsorption capacity of the metal ion in the single system. If there is no interaction between the metal ions the ratio should be 0.5. If adsorption is promoted by the presence of the other ion the ratio should be more than 0.5 and if the adsorption is hindered by the presence of the other ion the ratio should be less than 0.5.

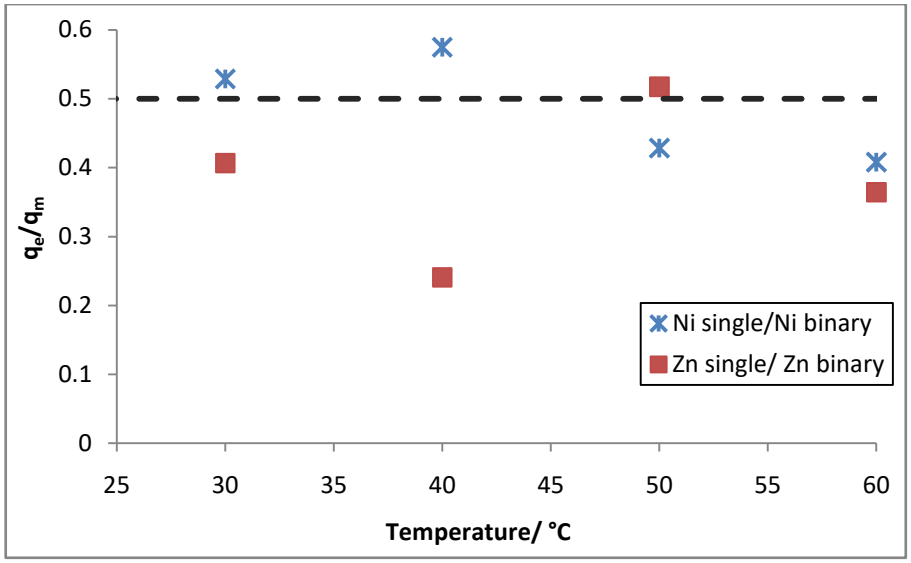

Figure 41. Equilibrium adsorption capacity ratios qe/qm against temperature for the nickel and zinc components of the binary system

According to Figure 41 in the presence of zinc ions the adsorption of nickel ions are promoted at lower temperatures while the presence of nickel reduce zinc adsorption at lower temperatures. At 60 °C the presence of other metal ions reduce the adsorption of both nickel and zinc. From this we can deduce that nickel and zinc are competitive in the binary environment.

4.8 Thermodynamic analysis of single system nickel, single system zinc and the binary system

The results were analysed using the Eyring equation (equation 16) where *ln*K was plot against 1/T to deduce the enthalpy, ΔH (kJ mol^{-1}), and entropy, ΔS ($kJmol^{-1}K^{-1}$), of a given system as shown in Figure 42. Gibbs free energy at each temperature for each system was calculated using the equilibrium constant k_d (Lg^{-1}). The Gibbs free energy, ΔG ($kJmol^{-1}$), is the thermodynamic potential of the process.

The more negative or less positive the Gibbs free energy is the more favoured the reaction is. The calculated parameters were summarised in Table 15.

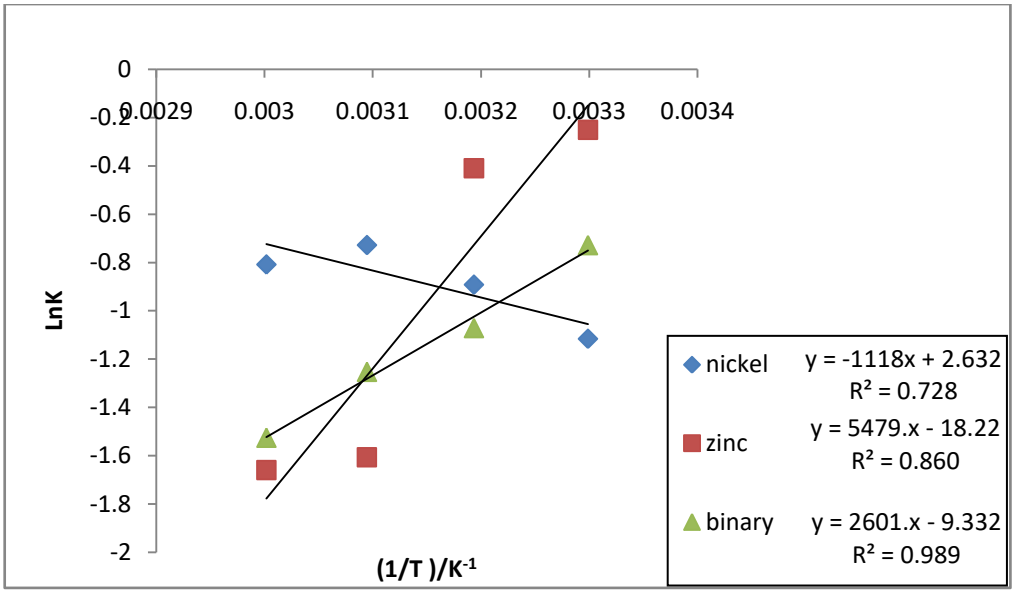

Figure 42. Arrhenius plot of the adsorption of nickel, zinc and the binary system

For adsorption in the zinc single system and the binary system the Gibbs free energy (ΔG) value becomes more positive as the temperature increases which means the adsorption is less favoured at higher temperatures. In the nickel single system ΔG value decreases as temperature increases until 60°C where it increases again which suggests the adsorption is promoted by higher temperatures but when the temperature is too high the adsorption becomes less favourable. The decrease in ΔG with temperature suggests that at the equilibrium desorption is favoured over adsorption at higher temperatures (Pandy et al. 2010). This is possibly due to the increase in solubility of the metal ions and the weakening of the metal ion-adsorbent bond as temperature increases.

The enthalpy (ΔH) and the entropy (ΔS) of the adsorption of nickel single system adsorption are both positive which mean the reaction is endothermic and there is an increase in entropy when the nickel ion binds to the adsorbent surface. The positive ΔS suggest the increase in entropy when the water around the metal ion and the adsorption site is displaced is more than the decrease in entropy when the metal ion binds to the adsorbent surface as shown in equation 25. Higher temperatures favour reactions with positive entropy which have dissociative mechanism. This was similar to results found by Ratan S. et al (2016) who found nickel adsorption to be

endothermic and entropically positive with adsorption increasing when the temperature was increased from 20°C to 50 °C. The ΔH and the ΔS of the adsorption of single system zinc is negative, which means the adsorption is exothermic and there is a decrease in entropy as the metal ions are less mobile than in solution when they are bound to the adsorbent. Nickel has a smaller charge density and ionic radius than zinc therefore more strongly binds to the water molecules when in solution so the decrease in the overall entropy when it is bound to the adsorbent surface is less than for zinc.

$$\boldsymbol{M^{2+}.(H_2O)_x + ROH.(H_2O)_y \leftrightharpoons ROM^{+} + H_3O^{+} + (x+y-1)H_2O} \quad \textit{Eq. 25}$$

The ΔH and ΔS of the adsorption in the binary system is very similar to the average of the ΔH and ΔS values of the nickel and zinc single systems being ΔH=-18.13 kJ mol^{-1} and ΔS= -0.06 $kJmol^{-1}K^{-1}$. The adsorption of the binary system is exothermic and has negative entropy which means it favours lower temperatures.

Table 15. Thermodynamic parameters for the adsorption of nickel and zinc in the single system and binary system, Co= 50 mg L^{-1}, adsorbent dose= 0.75 g

Parameters $\Delta G/kJmol^{-1}$	Nickel (single system)	Zinc (single system)	Binary system
30 °C	2.81	0.63	1.83
40 °C	2.32	1.06	2.79
50 °C	1.96	4.31	3.36
60 °C	2.24	4.59	4.22
ΔH/ kJ mol^{-1}	9.29	-45.55	-21.62
ΔS/ $kJmol^{-1}K^{-1}$	0.02	-0.15	-0.07

If ΔG is changes from negative to positive as the temperature increases as is the case for zinc, it means that adsorption is less favoured at higher temperatures. If the ΔG value is positive at all temperatures, as is the case for nickel single system and binary adsorption, it suggests that the adsorption requires some energy from an external source to occur (Saha et al. 2011).

4.9 Surface Analysis of Coir pith by Fourier Transform Infrared spectra – (FTIR)

The coir pith adsorbent was analysed using Fourier transform infrared spectra (FTIR) to deduce the functional groups on its surface. The FTIR measures the amount of infrared light absorbance (transmittance) by the surface. The more transmittance % deviates from 100 (which shows no absorbance) and the closer it is to 0% (total absorbance) the stronger the absorbance. Each functional group vibrates with a unique energy and will show absorbance in the corresponding wavenumber in the spectrum. The wider the peak the more unique vibrational modes the functional group has, for example the O-H bond has many vibrational modes and thus has a very wide peak. Coir pith was scanned in the wavelength range of 4000-800 cm^{-1} as shown in Figure 43. The FTIR analysis shows the presence of surface functional groups at their corresponding wavelengths; -OH (3000-3500 cm^{-1}), C-H (2900 cm^{-1}), C=O (1600 cm^{-1}), and C-O (1200-100 cm^{-1}). These peaks correspond to the polar groups of the lignin and cellulose of which coir pith is made of.

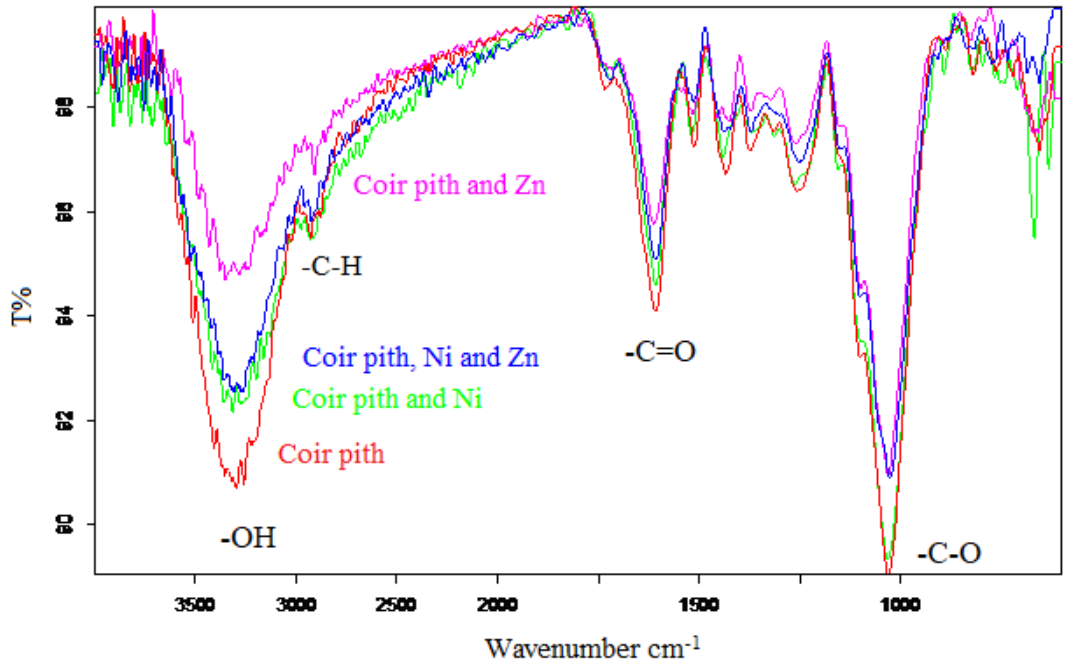

Figure 43. FTIR spectrum of coir pith (red), coir pith after being soaked in a 50 mgL^{-1} solution of zinc nitrate for 1 hour (purple), coir pith after being soaked in a 50 mgL^{-1} solution of nickel nitrate for 1 hour (green), coir pith after being soaked in a 50 mgL^{-1} solution of nickel nitrate and zinc nitrate for 1 hour (blue)

If the height of the functional group peak decreases after adsorption takes place this means there are less of this type of bond, possibly the metal ion has replaced a part of the functional group. If there was a shift in the peak after adsorption means that when the metal ion binds to the functional group, and electrons are diverted from the functional group to the metal ion, which would reduce the strength of bond and therefore the absorbance.

This was evident when comparing the spectra of the coir pith before and after adsorption, and easily observable so when comparing the –OH peak (3000-3500 cm^{-1}). The transmittance of the –OH group in the spectra of coir pith after zinc adsorption was much larger (smaller peak) when compared the spectra of coir pith before adsorption. This shows that there is a smaller concentration –OH bonds.

It is likely then when the metal ion forms a bond with the functional group; it replaces a hydrogen ion and forms a complex as shown in Figure 44. Similar change in this peak was observed in the spectra of coir pith after nickel adsorption and the spectra of coir pith after binary adsorption; however it was to a lesser extent. There was also a shift in the peak position to a lower wavenumber suggesting the energy of the bond and therefore the strength of the bonds were weaker.

In the spectra of coir pith after zinc adsorption the C-O and C=O peaks are smaller than in the spectra of coir pith before adsorption. The spectra of the binary system show similar changes at the C-O and C=O peaks but the spectra after nickel adsorption does not. This suggests the zinc interacts with the C-O bonds but nickel does not. This may also contribute to there being more zinc adsorption than nickel adsorption as zinc ions adsorb onto more sites than nickel ions.

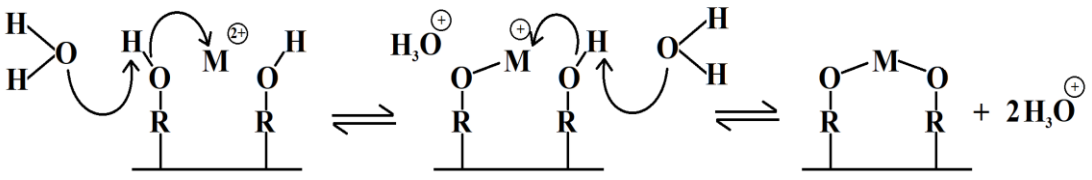

Figure 44. Mechanism of complexation of metal ions chemisorbing to the functional groups on the coir pith surface

CHAPTER 5: CONCLUSIONS

5.1 Conclusions

The conclusions of this study are as follows.

1. The reviewed literature provided an understanding of the adsorption process and the adsorbent to be used to remove heavy metals, as well as the need for this study.

2. The data from both the single systems were fit into the Langmuir, and Freundlich isotherm models. Nickel and zinc single systems fit both models satisfactorily.Howeverthe fit to the Freundlich model was better, highlighting that adsorption surface is heterogeneous.

3. The isotherm data from the binary system was fit to the Langmuir, Freundlich and extended Langmuir models.It fit only the Langmuir model satisfactorily highlighting a homogenous adsorption surface.

4. Results from the intraparticle diffusion analysis confirms the results of the Isotherm models as it shows at 30°C that there is intraparticle diffusion in the zinc and nickel single systems while there is no intraparticle diffusion in the binary system.

5. Most adsorption occurs at a higher pH value. To decrease costs and possibility of metal hydroxide precipitation the adsorption should be carried out at a neutral pH.

6. The kinetic data for single and binary system adsorption fit Lagergren pseudo second order model best, highlighting that the adsorption is mostly chemisorption.

7. Single system zinc adsorption and binary system adsorption decreased as the temperature increased.

8. In the single system, the adsorption of zinc at the lower temperatures is much higher than nickel at lower temperatures while in the binary system they have similar adsorption close to room temperature. Similar to the single system the adsorption of zinc decreases with temperature in the binary system as well.

9. The adsorption of nickel increases with temperature in the single system but decreases in the binary system.The adsorption of nickel is preferred to the adsorption of zinc at higher temperatures in the binary system.

10. The binary system adsorption capacity was less than the average of the single systems under similar conditions. Whereas percentage of nickel adsorption is more in the binary systems compared to percentage of nickel in the average of the single systems. This highlights the competitive nature of the binary system.

5.2 Future Recommendations

1. Test adsorption using continuous flow fixed-bed column as shown in Figure 45.

2. Test other parameters ex: low temperatures (5^{o}C< T< ^{o}C), effect of particle size

3. Study the effect of different ratios of nickel and zinc in solution

4. Introduce more metal ions and study the effects

5. Study the effect of introducing other counter ions or salts

6. Try different pre-treatments to the coir pith to increase adsorption or add more functional groups ex: carboxylic or sulfonic acid groups

7. Test ways to regenerate used adsorbent (remove adsorbed compounds)

REFERENCES

Abo-Ghander N. S., Rahman S. U.&Zaidi S. M. J. (2008) 'A Modified Electrodialytic Cell to Recover Heavy Metals from Wastewaster' PortugaliaeElectrochimicaActa 24, pp. 367-376

Agency for Toxic Substances and Disease Registry (ATSDR),(2005), Toxicological profile for Nickel. Atlanta, GA: U.S. Department of Health and Human Services, Public Health Service

Agnihotri, S.,Mota, J.P.B.,Abadi, M.R.& Rood, M.J, (2006), Theoretical and experimental investigation of morphology and temperature effects on adsorption of organic vapors in single-walled carbon nanotubes, J. Phys. Chem. B 110, pp. 7640–7647.

Ajmal M, Rao RAK, Ahmad J, Ahmad R (2006) 'The Use of Testa of Groundnut Shell (Arachis hypogea) for the Adsorption of Ni(II) from the Aqueous System.' Journal of Environ Science &Eng, 48, pp. 221-224.

Al-Enezi G., Hamoda, M. F. &Fawzi, N. (2004) 'Ion Exchange Extraction of Heavy Metals from Waste Water Sludges,' Journal of Environmental Science and Health, Part A, 39(2), pp. 455-464

Amarasinghe, B.M.W.P.K., (2007), 'Comparison of Adsorption Characteristics of Waste Biomass Materials for the Removal of Pb ions from Industrial Effluents,' Engineer: Journal of the Institution of Engineers, Sri Lanka, 40(4), pp.167–174.

Amarasinghe, B.M.W.P.K., (2011), 'Lead and Cadmium Removal from Aqueous Medium Using Coir Pith as Adsorbent: Batch Fixed bed Column Studies,' JTFE, 1(1), pp. 36-47

Anirudhan, T. S. &Sreekumari, S. S. (2011) Adsorptive removal ofheavy metal ions from industrial effluents using activatedcarbon derived from waste coconut buttons.JournalofEnvironmental Sciences,23(12), pp. 1989–1998

Annadurai G., Juang R.S., Lee D.J. (2002) 'Adsorption of heavy metals from water using banana and orange peels,' Water Science and Technology. IWA Publishing 47, pp. 185-190

Babel, S. &Kurniawan, T. A. (2004) Cr (VI) removal from syntheticwastewater using coconut shell charcoal and commercialactivated carbon modified with oxidizing agents and/orchitosan.Chemosphere,54(7), pp. 951–967

Bakalár T., Búgel M., Gajdošovā L., (2009) 'Heavy metal removel using reverse osmosis,' ActaMontanisticaSlovaca, 14(3), pp. pp. 250-253

Bhattacharyya, S., Lelong, G. &Saboungi, M. L. (2006) Recentprogress in the synthesis and selected applications of MCM-41: a short review.Journal of Experimental Nanoscience1(3), pp. 375–395

Charerntanyarak L. (1999) Heavy Metal Removel by Chemical Coagulation and precipitation, Water Science and Technology, 39(10), pp. 135-138

Cheung WH, Szeto YS, &McKay G (2007) 'Intraparticle diffusion processes during acid dye adsorption onto chitosan,' *BioresourTechnol*, 98, pp.2897–2904

Choi, H. J., Yu, S. W. & Kim, K. H. (2016) Efficient use of Mg-modified zeolite in the treatment of aqueous solutioncontaminated with heavy metal toxic ions.Journal of theTaiwan Institute of Chemical Engineers63, pp. 482–489.

Conrad, K., and Hansen, H. C. B., (2007), 'Sorption of zinc and lead on coir,' Bioresource Technology, 98(1), pp.89-97.

Conrad, K.; Hansen, H.C.B. (2007) 'Sorption of zinc and lead on coir.' Bioresource Technol., 98, pp. 89-97.

Dąbrowski A., Hubicki Z., Podkościelny P., Robens E. (2004) 'Selective removal of the heavy metal ions from waters and industrial wastewater by ion exchange method' Chemosphere 56(2), pp. 91-106

Dai, H., (2002), Carbon nanotubes: opportunities and challenges, Surf. Sci. 500, pp. 218–241.

El Samrani A.G., Lartiges B. S., &Villiéras F., (2008), 'Chemical Coagulation of combines sewer overflow: Heavy metal removal and treatment optimization,' Water Research, 42(4), pp. 951-960

Ewecharoen, A., Thiravetyan, P., and Nakbanpote, W. (2008) "Comparison of nickel adsorption from electroplating rinse water by coir pith and modified coir pith," Chemical engineering journal, 137, pp. 181-188

Fernando, A., Monteiro, S., Pinto F., and Mendes B., (2009) 'Production of Biosorbents from Waste Olive Cake and Its Adsorption Characteristics for Zn2+Ion' Sustainability, 1, pp.277-297

Freundlich, H.M.F., (1906) 'Über die adsorption in lo¨sungen (Adsorption in solution),' *J. ChemPhys*, 57, pp. 384–470

Friberg L., Norberg G. F.,&Vouk V. B., eds. (1986) Handbook of the Toxicology of Metals Vol. II Amsterdam, Elsevier, pp. 130-189

Gonzalez M. H., Araùjo G. C. L., Pelizaro C. B., Menezes E. A., Lemos S. G., Batista de Sousa G., Nogueira A. R. A., (2008), 'Coconut coir as biosorbent for Cr(VI) removal from laboratory wastewater,' Journal of Hazardous Materials, 159(2-3), pp. 252-256.

Gopalakrishnan, A., Krishnan, R., Thangavel, S., Venugopal, G. &Kim, S. J. (2015), Removal of heavy metal ions from pharma-effluents using 71rapheme-oxide nanosorbents and study oftheir adsorption kinetics.Journal of Industrial andEngineering Chemistry30, pp.14–19

Gosset T., Trancart J. L., Thevenot D.R. (1986) 'Batch metal removal by peat.' Water Res 20, pp. 21-26.

Halsey G. D. (1952), 'The role of surface heterogeneity,' *Adv. Catal*, 4, pp.259-269

Hawari A.H., Mulligan C.N., (2006), 'Biosorption of lead(II), cadmium(II), copper(II) and nickel(II) by anaerobic granular biomass,' Bioresour. Technol. 97 (4), pp. 692–700.

Hidayat, H., and Yoyon S. (2014) 'Zinc Adsorption Kinetics Using Pseudomonas as Biomass.' Biopropal Industri, 5(1), pp. 37-43

Ho, Y. S. (1995), 'Adsorption of heavy metals from waste streams by peat,' *Ph.D. thesis, University of Birmingham, Birmingham, UK.*

Ho, Y. S., and McKay, G. (1998) 'A comparison of chemisorptions kinetic models applied to pollutant removal on various sorbents,' *Trans IchemE*, 76(B), pp. 332-339

Ho, Y. S., and McKay, G. (1999) 'Competitive Sorption of Copper and Nickel Ions from Aqueous Solution Using Peat,' *Adsorption*, 5, pp. 409-417

Hui, K. S., Chao, C. Y. H. &Kot, S. C. (2005) Removal of mixedheavy metal ions in wastewater by zeolite 4A and residualproducts from recycled coal Fly ash.Journal of HazardousMaterials127(1), 89–101.

IUPAC, Compendium of Chemical Terminology, 2nd ed. (the "Gold Book") (1997).Online corrected version: (2006–) "transition element".

Jablonovská K. and Štyriaková, I, (2006) 'Adsorption of zinc and lead on clay minerals' Acta Montanistica Slovaca, 11(2),pp. 304-308

Kadirvelu, K., and Namasivayam, C., (2003), 'Activated carbon from coconut coirpith as metal adsorbent: adsorption of Cd(II) from aqueous solution,' Advanced in Environmental Research, 7(2), pp. 471-478.

Kalavathy, M.H.; Karthikeyan, T.; Rajgopal, S.;& Miranda, L.R., (2005), Kinetic and isotherm studies of Cu (II) adsorption onto H3PO4-activated rubber wood sawdust. J. Colloid Interface Sci., 292, pp.354–362.

Karthikeyan, T., Rajgopal, S. & Miranda, L. R. (2005) Chromium(VI) adsorption from aqueous solution by HeveaBrasilinesissawdust activated carbon.Journal of Hazardous Materials124(1), pp. 192–199.

Khalfaoui, M., Knani, S., Hachicha, M. A. & Ben Lamine, A., (2003), 'New theoretical expressions for the five adsorption type isotherms classified by BET based on statistical physics treatment,' *J. Colloid Interface Sci.*, 263(1), pp.350-356

Krikorian, N. & Martin, D. F. (2005) Extraction of selected heavy metals using modified clays. Journal of Environmental Science and Health 40 (3), pp. 601–608.

Kumar, K. V., Ramamurthi, V., &Sivanesan, S., (2005), 'Modeling the mechanism involved during the sorption of methylene blue onto fly ash,' *J. Colloid Interface Sci.*, 284(1), pp.14-21

Lagergren, S., (1898), 'About the theory of so-called adsorption of soluble substances.'*KungligaSvenskaVetenskapsakademiens. Handlingar*, 244, pp. 1–39

Langmuir, (1916), 'The constitution and fundamental properties of solids andliquids,' *J. Am. Chem. Soc*. 38, pp.2221–2295.

Lo, S. F., Wang, S. Y., Tsai, M. J. & Lin, L. D. (2012) Adsorptioncapacity and removal efficiency of heavy metal ions by Mosoand Ma bamboo activated carbons.ChemicalEngineeringResearch and Design90(9), pp. 1397–1406.

Malkoc, E., Nuhoglu Y. (2005) 'Investigations of Nickel (II) Removal from Aqueous Solutions Using Tea Factory Waste.' Journal of Hazardous Materials B 127, pp. 120-128.

Nasrullah, A., Bhat, A. H., Isa, M. H., (2016) 'Lignin: A sustainable biosorbent for heavy metal adsorption from wastewater, a review,' AIP Conference Proceedings 2016

National Environmental (Protection and Quality) Regulations, No. 1 of 2008.

Oura, K., Lifshits, V.G., Saranin, A.A., Zotov, A.V., Katayama, M. (2003). Surface Science, An Introduction, Springer.

Pandey, P.K., Sharma, S.,&Sambi, S., (2010), Kinetics and equilibrium study of chromium adsorption on zeoliteNaX. Int. J. Environ. Sci. Tech, 7(2), pp. 395-404.

Rahman, I. A., Ismail, J. & Osman, H. (1997) Effect of nitric acid digestion on organic materials and silica in rice husk. Journal of Materials Chemistry 7 (8), 1505–1509

Ramos,S. N. D. C., Xavier,A. L. P., Teodoro, F. S., Elias, F. J., Goncalves, L,, Gil,L. F., de Freitas,R. P.,&Gurgel,L. V. A.,(2015) "Modeling mono- and multi-component adsorption of cobalt (II), copper (II), and nickel (II) metal ions from aqueous solution onto new carboxylate sugarcane bagasse. Part I: Batch adsorption study, Industrial Crops and Products, Volume 74, pp. 357-371,

Ratan S, Singh I, Sarkar J, Naik RM (2016) The Removal of Nickel from Waste Water by Modified Coconut Coir Pith. ChemSci J 7: 136.

Reddad, Z. G´erente, C. Andr`es, Y. Ralet, M.C. Thibault, J.-F. Cloirec, P.L. (2002) 'Ni(II) and Cu(II) binding properties of native and modified sugar beet pulp,' Carbohydr. Polym. 49 (1), pp.23–31.

Reddad, Z.;Gerente, C.;Andres, Y.;Le-Cloirec P. (2002) 'Adsorption of Several Metal Ions onto a Low-Cost Biosorbent: Kinetic and Equilibrium Studies.' Environ. Sci. Technol., 36, pp.2067-2073

Saeed, A.; Akhter, M.W., Iqba, M., (2005) 'Removal and recovery of heavy metals from aqueous solution using papaya wood as a new biosorbent.' Separation and Purification Technology, 45, pp.25-31.

Saha, P., &Chowdhury, S., (2011). Insight Into Adsorption Thermodynamics, Thermodynamics, Prof. Mizutani Tadashi (Ed.), ISBN: 978-953-307-544-0, InTech,

Saleem, M. and Kazi, GH. (1998). 'Concentration and distribution of heavy metals (lead, cadmium, chromium, copper, nickel, zinc) in Karachi shore and offshore sediments.' Pakistan Journal of Marine Sciences. 7(1), pp.71-79

Sdiri, A. T., Higashi, T., &Jamoussi, F., 'Adsorption of copper and zinc onto natural clay in single and binary systems,' *Int. J. Environ. Sci. Technol.* (2014) 11, pp.1081–1092

Shaheen, S. M., Derbalah, A. S., &Moghanm F.S., (2012) 'Removal of Heavy Metals from Aqueous Solution by Zeolite in Competitive Sorption System,' *IJESD*, 3(4), pp. 362-367

Sharifipour, F., Hojati, S., Landi, A. &Faz Cano, A. (2015) 'Kinetics and Thermodynamics of Lead Adsorption from Aqueous Solutions Onto Iranian Sepiolite and Zeolite,' *Int. J. Environ. Res.*, 9(3), pp.1001-1010.

Shukla, S.R.; Pai, R.S. (2005) 'Adsorption of Cu (II), Ni (II) and Zn(II)on dye loaded groundnut shells and sawdust.' Sep. Purif.Technol., 43, pp.1-8.

Singh, S. P., Ma, L. Q. & Harris, W. G. (2001) 'Heavy metal interactions with phosphatic clay.' Journal of Environmental Quality 30 (6), 1961–1968.

Singhe, N., &Balomajumder, C., (2017) 'Equilibrium isotherm and kinetic studies for the simulataneous removal of phenol and cyanide by use of S. Odorifera (MTCC 5700) immobilized on coconut shell activated carbon,' *Appl Water Sci*. 7 pp.3241-3255.

Suksabye P, Nakajima A, Thiravetyan P, Baba Y, Nakbanpote W. (2009) 'Mechanism of Cr(VI) adsorption by coir pith studied by ESR and adsorption kinetic.' Journal of Hazardous Materials, 161(2–3), pp. 1103–1108

Suksabye P, Thiravetyan P, Nakbanpote W, Chayabutra S. (2007), 'Chromium removal from electroplating wastewater by coir pith,' Journal of Hazardous Materials, 141(3), pp.637-644.

Y. T. Ong, A. L. Ahmad, S. Hussein, S. Zein, and S. H. Tan,(2010), "A review on Carbon Nanotubes in an Environmental Protection and Green Engineering Perspective," Brazilian J. Chem. Eng., vol. 27, no. 2, pp. 227–242.

Taha G. M. (2006) 'Utilization of Low-Cost Waste Material Bagasse Fly Ash in Removing of Cu2+, Ni2+, Zn2+, and Cr3+ from Industrial Waste Water.' Ground Water Monitoring & Remediation, 26, pp. 137-141.

Taylor, P., Lan, Y., Wang, Y.,&Ren,Z. F., (2011) "Physics and applications of aligned carbon nanotubes," in Advances in Physics, 2011, pp. 553–678.

Thangavel, S. &Venugopal, G. (2014) Understanding the adsorption property of 74rapheme-oxide with different degrees of oxidation levels. Powder Technology257, pp. 141–148.

Villaescusa, I. Fiol, N. Mart´ınez, M. Miralles, N. Poch, J. Serarols, J. (2004) 'Removal of copper and nickel ions from aqueous solutions by grape stalks wastes,' Water Res. 38 (4), pp. 992–1002.

Wahyuni E.T, Aprilita N.H., Hatimah H., Wulandari A.M., Mudasir M., (2015) 'Removal of Toxic Heavy Metal ions in water by Photocatalytic Method, American Chemical Science Journal, 5(2), pp. 194-201.

Wijayawardhana, D., Herath, V. and Weerasinghe, A. (2016) 'Heavy Metal Pollution in Sri Lanka with Special Reference to Agriculture: A review of current research evidence,' *Rajarata University Journal*, 4(1) pp. 52-66.

Wijeyaratne W.M. D. N. (2016) 'Application of pollution indices to quantify the pollution status of shallow sediments of the Bolgoda Lake, Sri Lanka. J.Natn.Sci.Foundation Sri Lanka.' 44 (3), pp. 279-289

Wingenfelder U., Hansen C., Furrer G., &Schulin R. (2005) 'Removal of Heavy Metals from Mine Waters by Natural Zeolites' Environ. Sci. Technol., 39, pp. 4606-4613

Wyszkowska J., Borowil A., Kucharski M., Kucharski J, (2012) Effect of cadmium, copper, and zinc on plants, soil microorganisms and soil enzymes. Journal of Elementology 18, pp. 769-796.

Zendelska A., Mirjana Golomeova, M, Blazev, K., Krstev B., Golomeov B., and Krstev, A., (2014) 'Equilibrium Studies of Zinc Ions Removal from Aqueous Solutions by Adsorption on Natural Zeolite' Journal of Materials Science and Engineering A, 4 (7), pp. 202-208

Appendix

Determination of particle density, bulk density and porosity

W1 - weight of specific gravity bottle
W2 - weight of specific gravity bottle+ coir pith weight
W3 - weight of specific gravity bottle+ coir pith weight+ weight of oil
W4- weight of specific gravity bottle+ weight of oil
W5- weight of specific gravity bottle+ water

Density=mass/volume
Mass of coir pith= (W2-W1)
Volume of coir pith= volume of bottle- volume of oil
Volume of bottle= (W5-W1) as density of water= 1 g/cm^3
Volume of oil in W3= Mass of oil/ density of oil= (W3-W2)/density of oil
Density of oil= $(\frac{W4-W1}{W5-W1})$
Volume of oil in W3= $\frac{(W3-W2)(W5-W1)}{(W4-W1)}$
Volume of coir pith= (W5-W1)-$\frac{(W3-W2)(W5-W1)}{(W4-W1)}$= $\frac{(W5-W1)(W4-W1)-(W3-W2)(W5-W1)}{(W4-W1)}$
Density of coir pith= $\frac{(W2-W1)(W4-W1)}{(W5-W1)(W4-W1)-(W3-W2)(W5-W1)}$= $\frac{(W2-W1)(W4-W1)}{(W5-W1)((W4-W1)-(W3-W2))}$

	1	2	3
W1	19.0229	19.0211	19.0365
W2	21.1809	20.5177	20.3763
W3	62.9540	63.3598	63.3569
W4	64.6401	64.6056	64.5735
W5	68.7292	68.6885	68.6851
Coir pith density /g cm^{-3}	0.5104	0.49999	0.48069

Average= 0.497 g cm^{-3}

Bulk density

	1	2	3
Mass of cylinder/ g	44.3158	44.3142	44.3057
Mass of cylinder + coir pith /g	45.2639	45.5892	45.1704
Volume of coir pith /cm^3	9	9	9
Bulk density / g cm^3	0.1053	0.1416	0.0961

Average= 0.1143 g cm^{-3}

Porosity =1-(bulk density/particle density) = 1-(0.1143/0.497)= 0.77

Calculation for the preparation of the nickel and zinc stock solutions of concentration 1 g/L

Zinc nitrate hexahydrate (Zn(NO3)2.6H2O)
Molar mass – 235.474 g/mol
Atomic mass of zinc- 65.38 g/mol
Mass of zinc nitrate hexahydrate which contains 1 g of zinc-235.474/65.38= 3.60 g

Nickel nitrate hexahydrate (Ni(NO3)2.6H2O)
Molar mass – 290.791 g/mol
Atomic mass of nickel- 58.693 g/mol
Mass of zinc nitrate hexahydrate which contains 1 g of nickel- 290.791/58.693= 4.95 g

Table of dilutions for solutions of different concentrations of adsorption isotherm study

Single system nickel/zinc concentration

	Stock solution/ cm^3	Distilled water/ cm^3	Concentration/ mg L^{-1}
1	5	495	10
2	10	490	20
3	25	475	50
4	50	450	100
5	100	500	200

Binary system nickel and zinc

	Stock solution of nickel/ cm^3	Stock solution of zinc/ cm^3	Distilled water/ cm^3	Concentration/ mg L^{-1}
1	2.5	2.5	495	10
2	5	5	490	20
3	12.5	12.5	475	50
4	25	25	450	100
5	50	50	500	200

Particle size distribution calculation

Fraction	Coir pith mass/g	% of total mass

1 mm - 710 µm	13.3384	47%
710 µm - 500 µm	9.5462	34%
500 µm - 335 µm	5.4498	19%
Total	28.3344	

Maximum adsorption capacity calculated using equation 4.1 and values derived from the Freundlich constants

Initial Concentration (C_o)/ mg L^{-1}	q_{max}		
	Nickel	Zinc	Binary
2.5	5.398749	5.151901	7.829193
5	6.786299	7.43898	8.567437
10	8.530469	10.74136	9.375292
20	10.72291	15.50976	10.25932
50	14.50885	25.20655	11.55715
100	18.23782	36.39647	12.64692
200	22.92518	52.55393	13.83945

Analysis of zinc adsorption by Lagergren Pseudo first order model at 30, 40, 50, and 60 °C

Temp/°C	Graphical method			Data fitting			Experimental qe
	q_e	K_1	R^2	q_e	K_1	R^2	
30	14.67	0.23	0.863	17.55	0.314	0.75	17.94
40	9.57	0.56	0.79	15.69	1.84	0.38	16.5
50	-	-	-	10.62	19.18	0	7.73
60	-	-	-	10.34	19.13	0	7.40

Analysis of zinc adsorption by Lagergren Pseudo second order model at 30, 40, 50, and 60 °C

Temp/ °C	Graphical method			Data fitting method			Experimental qe
	q_e	k_2	R^2	q_e	k_2	R^2	
30	18.52	0.034	0.99	18.57	0.028	0.99	17.95
40	16.94	0.145	0.99	16.26	0.25	0.57	16.63
50	7.35	-0.05	0.99	9.157	-0.302	0.68	7.73
60	7.407	-0.049	0.99	9.602	-0.493	0.16	7.41

Analysis of binary adsorption by Lagergren Pseudo first order model at 30, 40, 50, and 60 °C

Temp/ °C	Graphical method			Data fitting method			Experimental qe
	q_e	k_2	R^2	q_e	k_2	R^2	
30	14.084	0.031	0.99	11.622	-0.528	0.29	14
40	11.494	-0.138	0.99	12.24	0.191	0.38	11.34
50	9.9	-0.027	0.99	15.3	-0.307	0.174	9.99
60	6.578	-0.026	0.99	15.58	-0.204	0.246	6.67

Analysis of binary adsorption by Lagergren Pseudo second order model at 30, 40, 50, and 60 °C

Temp/ °C	Graphical method			Data fitting method			Experimental qe
	q_e	k_2	R^2	q_e	k_2	R^2	
30	18.52	0.034	0.99	18.57	0.028	0.99	17.95
40	16.94	0.145	0.99	16.26	0.25	0.57	16.63
50	7.35	-0.05	0.99	9.157	-0.302	0.68	7.73
60	7.407	-0.049	0.99	9.602	-0.493	0.16	7.41